To the Graduate Council:

I am submitting herewith a thesis written by Angelia Kaye Moore entitled "In-Situ Monitoring of the Deposition of Superconducting Thin Films by FT-IR and Mass Spectrometry." I have examined the final copy of this thesis for form and content and recommend that it be accepted in partial fulfillment of the requirements for the degree of Master of Science, with a major in physics.

James R. Thompson, Major Professor

We have read this thesis and
recommend its acceptance:

Accepted for the Council:

Associate Vice Chancellor
and Dean of The Graduate School

STATEMENT OF PERMISSION TO USE

In presenting this thesis in partial fulfillment of the requirements for a Master's degree at The University of Tennessee, Knoxville, I agree that the library shall make it available to borrowers without special permission, provided that accurate acknowledgement of the source is made.

Permission for extensive quotation from or reproduction of this thesis may be granted by my major professor, or in his absence, by the Head of Interlibrary Services when, in the opinion of either, the proposed use of the material is for scholarly purposes. Any copying or use of the material in this thesis for financial gain shall not be allowed without my written permission.

Signature Angelia K. Moore

Date Feb. 26, 1993

IN-SITU MONITORING OF THE DEPOSITION OF SUPERCONDUCTING THIN FILMS BY FT-IR AND MASS SPECTROMETRY

A Thesis

Presented for the

Master of Science

Degree

The University of Tennessee, Knoxville

Angelia Kaye Moore

May 1993

ACKNOWLEDGEMENTS

My sincere thanks to those who served as my committee members - Dr. J.R. Thompson, Dr. T.A. Callcott, and Winston Chen, who also served as my research advisor. Thanks to Sherrie Sharp for providing SEM photos of some of my films, and to Shen Zhu for x-ray diffraction analysis, additional resistance measurements, and many valuable discussions and suggestions. I would also like to thank Ron Phillips and Steve Allman for technical assistance and advice, and Dr. Marianne Breinig and Roy Buhl for encouragement and support.

ABSTRACT

Superconducting thin films were produced by pulsed laser ablation of a $YBa_2Cu_3O_{7-x}$ pressed pellet target, using a Nd:YAG laser operating at 1060, 532, 355, and 266 nm wavelengths. Various laser fluences from 20 to 0.5 J/cm^2 were used in order to study the effect of laser fluence and laser wavelength on film quality. Optimum laser fluence was 3 J/cm^2 for all wavelengths, while the best films were produced at shorter wavelengths. Fourier transform infrared (FT-IR) reflectance spectroscopy was used *in-situ* to observe the film deposition process. Quadrupole mass spectra were obtained independently, with the same laser fluences and wavelengths used previously. Typically, higher fluences produced fewer metal oxide ions, and stoichiometry was not preserved by the ablated positive ions. More Ba^+ ions than Y^+ or Cu^+ ions were observed. No CuO^+ ions were detected. SEM photographs revealed that longer wavelengths produced larger particle sizes in the films, and higher fluences produced the same results.

TABLE OF CONTENTS

LIST OF FIGURES

CHAPTER 1

INTRODUCTION

Superconductivity was discovered by a Dutch physicist named Kamerlingh Onnes in 1911. He found that as a mercury wire was cooled to a temperature of 4.2 Kelvin, its electrical resistance dropped to zero. The implications of his discovery were obvious to him: a material which has no resistance could carry current for long distances with no losses. Later, in 1933, Walter Meissner discovered that the class of metals which display superconductivity at low temperatures - superconductors - will not allow magnetic fields to penetrate them. The superconductors set up screening currents within which cancel the magnetic field and leave a zero net field inside the material. Also, when a superconductor is placed in a magnetic field and then cooled, the screening currents which are produced expel the magnetic field [1].

The discovery of high T_c superconductivity by Bednorz and Müller [2] began research into the properties of bulk metal oxide superconductors. One of the most promising new materials discovered, $YBa_2Cu_3O_{7-x}$, has a critical temperature above liquid nitrogen temperature [3]. A diagram of the crystal structure is shown in Figure 1 [4]. $YBa_2Cu_3O_{7-x}$ is a triply-layered oxygen-deficient perovskite which is either tetragonal or orthorhombic in structure depending on the oxygen content [5]. At high temperatures (above 700 °C), it is tetragonal while at lower temperatures (below 500 °C), it is

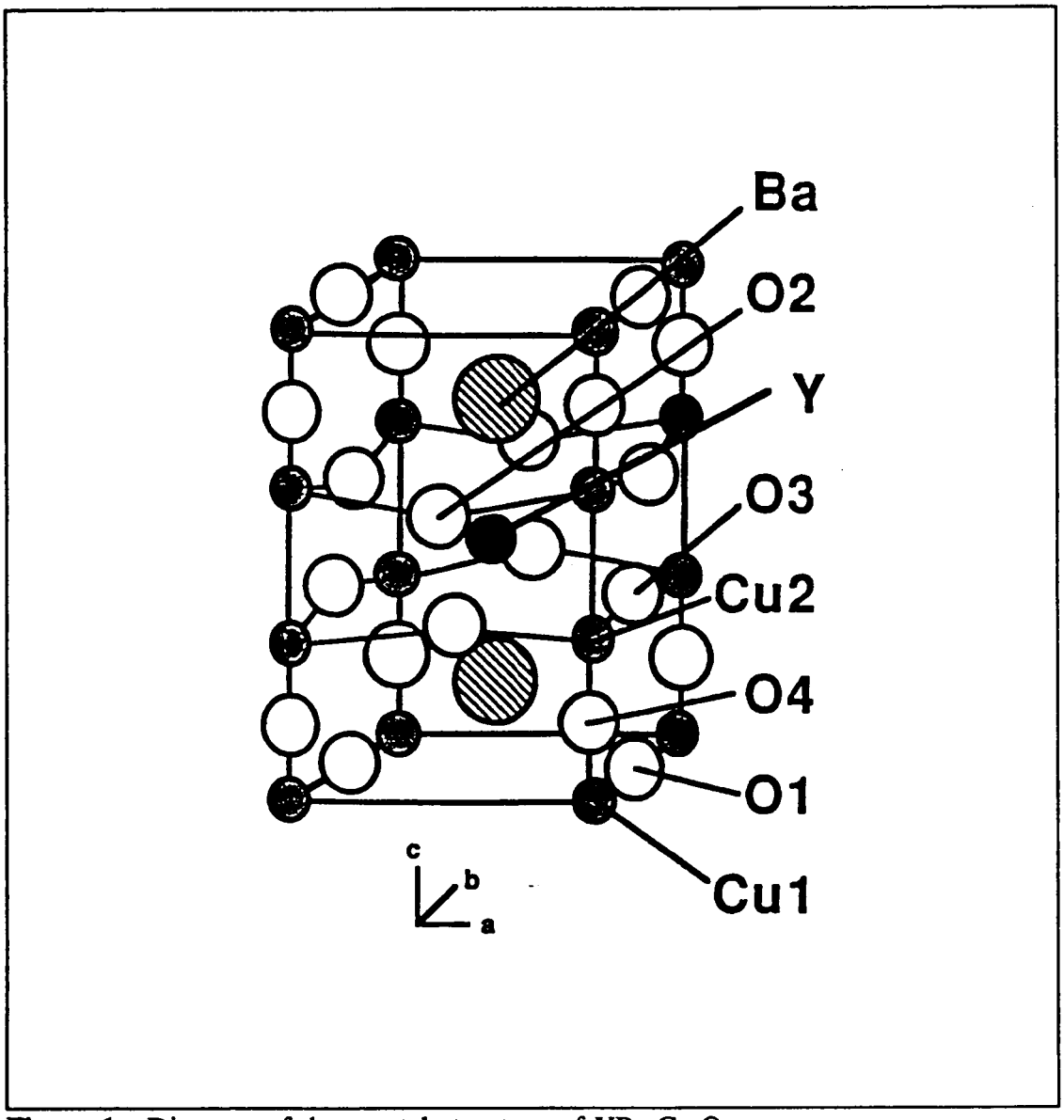

Figure 1. Diagram of the crystal structure of $YBa_2Cu_3O_{7-x}$.

Source: I-Wei Chen, *et al.*, "Superconductivity and the Tailoring of Lattice Parameters of the Compound $YBa_2Cu_3O_x$," Advanced Ceramic Materials, Special Supplementary Issue: Ceramic Superconductors, vol. 2, no. 3B, American Chemical Society, p. 466 (1987).

orthorhombic. This seems to be due to the fact that the oxygen vacancies are ordered along one of the basal axes of the molecule. When the vacancies are more ordered, the critical temperature tends to be higher.

Superconducting thin films of $YBa_2Cu_3O_{7-x}$ were successfully deposited on various (100) oriented substrates by pulsed laser ablation. Annealing in an oxygen environment was necessary to make them superconductive [6]. That was necessary because the deposited films were both oxygen deficient and not oriented with respect to the substrate, as determined by Rutherford backscattering spectra in channeling mode and x-ray diffraction measurements [7]. Research found that when the substrate temperature is 760 °C or above, $YBa_2Cu_3O_{7-x}$ films have c-axis orientation when produced on (100) oriented substrates [8]. Epitaxially ordered films have better paths for superconductivity and lower values for resistance [9]. That is due to the anisotropic conductivity of the superconductor; that is, the currents travel more easily in the a-b planes than currents along the c-axis [10]. For superconducting thin films produced by laser ablation, it was found that shorter wavelength lasers and shorter pulses are advantageous because they reproduce on the substrate the stoichiometry of the target material [11].

One of the substrates being used for superconducting thin film deposition is lanthanum aluminate ($LaAlO_3$), which can be prepared as a (100) oriented single crystal. This material makes a good lattice match with the basal plane of the $YBa_2Cu_3O_{7-x}$ film, which is important to reduce thermal strain. Also, substrate-film interaction seems to be negligible. Thin films deposited on $LaAlO_3$ substrates typically have a T_c ranging from approximately 84 K [12] to 90 K [13].

Superconducting materials hold great promise in electronics, provided that the critical temperature can be increased significantly. Since superconducting wires have no resistive losses, electricity could be carried over long distances with greatly improved efficiency and substantial monetary savings. The other benefit of using superconductors, the fact that no heat is generated when current is sent through the wire, would enable the components in an integrated circuit to be placed closer together and reduce further the size of computers and other devices. Currently, superconductors are used in magnetic resonance imaging (MRI) for medical diagnosis and in the construction of the Superconducting Supercollider. The refrigeration systems for the old type metallic alloy superconductors used in these devices are quite expensive because they require liquid helium to reach their very low critical temperatures. Oxide superconductors using liquid nitrogen would be much less expensive to operate, but the problems associated with these high-T_c materials, namely oxygen loss, brittle and inflexible structure, and sensitivity to magnetic fields, have yet to be solved.

It is necessary to perfect thin film deposition of superconducting materials because bulk superconductors are too brittle to use in electronics. The films could be deposited on metallic wires in order to utilize their superconducting properties and improve their flexibility and durability. Research is presently aimed at lowering substrate temperature during deposition of superconducting thin films. Low temperatures reduce the chemical reactions between the substrate and the film [14]. In addition, the films are smoother and less granular than films deposited at higher temperatures [15]. It is hoped that eventually

$YBa_2Cu_3O_{7-x}$ superconducting thin films can be deposited directly on silicon at low substrate temperatures to avoid decomposition and allow use in integrated circuits.

The role of oxygen in superconductive thin film preparation is not well understood. The observation of trapped O_2 in high-T_c superconductors [16] could play an important role in the mechanism of superconductivity. It has been proposed that an *in-situ* monitoring system might reveal the importance of oxygen, in particular, why oxygen gas is required during preparation of films (and bulk material) and why it tends to diffuse out of the film after a period of time. Supposedly, the laser energy is energetic enough to activate the oxygen and increase its reactivity [17]. It has been noted that the chemical analysis of $YBa_2Cu_3O_{7-x}$ samples show a higher oxygen content than the analysis of neutron diffraction techniques [18]. The importance of observing the deposition process while it is taking place is critical. There are several different methods being used to monitor film growth *in-situ*: Rutherford backscattering (RBS), x-ray diffraction (XRD), scanning electron microscope (SEM), reflection high energy diffraction (RHEED), and Fourier transform infrared spectroscopy (FT-IR). Of all of these methods, FT-IR is the most convenient and most cost-efficient. Mass spectrometer analysis could be used to determine if stoichiometry is being preserved and Fourier transform infrared (FT-IR) reflectance spectroscopy can be used as a method of determining film thickness, morphology, and crystalline phase. In addition, FT-IR emission spectroscopy can be used to determine the surface temperature of the substrate [19].

The details of the kinematics of laser ablation are not well known at this time. The different methods described previously--FT-IR reflectance spectroscopy and mass spectroscopy--should help form an understanding of what type of particles are ejected from the superconducting target, how particles ablated from the target are deposited on the substrate, and what effect heating and oxygen incorporation have on film quality.

CHAPTER 2

EXPERIMENTAL PROCEDURE

A diagram of the equipment used for film deposition and *in-situ* monitoring is shown in Figure 2. This experiment used a Quanta-Ray DCR Nd:YAG laser operating at 10 Hz with an HG-2 harmonic generator which was capable of producing wavelengths of 1060, 532, 355, and 266 nm. An NRC Newport Corp. Model 935-10 attenuator was used to attenuate the laser energy. A Scientech 362 power energy meter measured the laser energy. A vacuum chamber with substrate heater (Barber-Colman 520 solid state controller) and a target holder which was rotated by computer control (Compumotor microstep drive AX Series) were used for film deposition. A BOMEM Michelson MB Series interferometer with an Infrared IOH-1093 MCT detector obtained FT-IR reflectance spectra of the film during deposition.

The film deposition proceeded as follows: first, the detector was cooled with liquid nitrogen and the spectrometer and detector alignment was checked by computer using Lab-Calc computer software. A 10 mm x 10 mm x 1 mm piece of single crystal (100) orientation lanthanum aluminate (Atomergic Chemicals) was firmly attached to the substrate heater with silver paint. A thin sheet of aluminized mylar was stretched tightly over the surface of the substrate and held in place. An FT-IR reference spectrum was taken with the chamber in the 10^{-7} to 10^{-6} Torr range, using the aluminized mylar as a

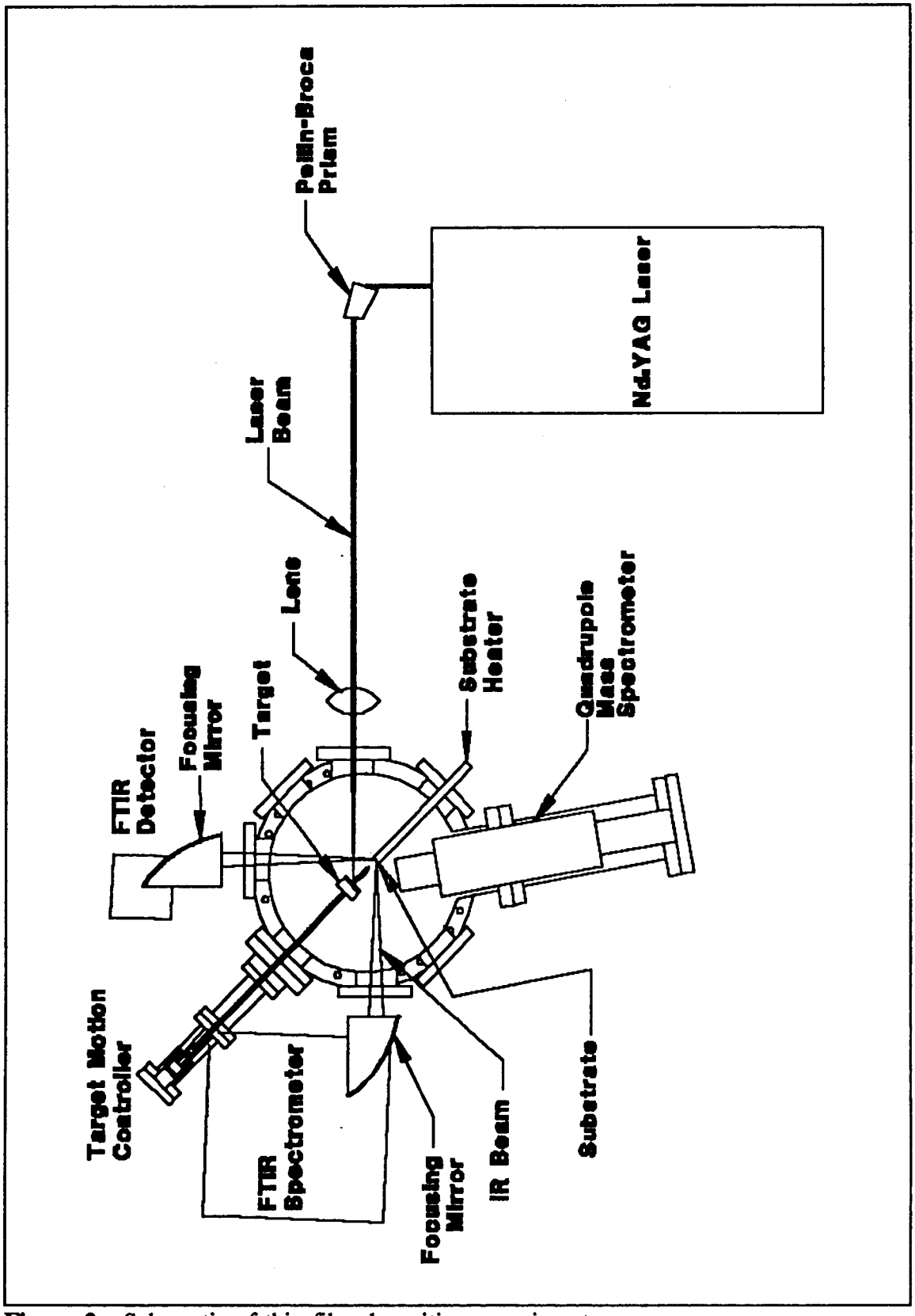

Figure 2. Schematic of thin film deposition experiment.

mirror. The interferometer was set for mid IR, 150 scans, and a resolution of 8 cm^{-1}. The initial intensity of light reflected from the aluminized mylar is used as a reference. A typical reference spectrum is shown in Figure 3. The absorption bands are due to CO_2 and water. During alignment and while taking references, two metal screens were placed in front of the infrared detector to avoid saturation of the signal. The chamber was then backfilled to 1 atm with O_2 gas, the aluminized mylar was removed while the substrate remained in place, and the chamber pumped down again.

After the chamber pressure reached approximately 1 x 10^{-5} Torr, both the turbo pump and roughing pump were valved off. A Baratron gauge was used to introduce 200 milliTorr O_2 gas into the chamber, and FT-IR spectra were taken at room temperature, 400, 600, and 760 °C. It was discovered that without this background oxygen present, films produced by laser ablation were brown, transparent, and oxygen deficient [6]. Apparently, the oxygen prevents decomposition of the tetragonal $YBa_2Cu_3O_{7-x}$ [20]. The $LaAlO_3$ references before division by the mirror reference are shown in Figure 4. $LaAlO_3$ references after division by the mirror reference are shown in Figure 5. The trace with the greatest relative intensity was taken at room temperature, the one with next highest intensity corresponds to 400 °C, the next one was taken at 600 °C, and the trace with lowest relative intensity was taken at 760 °C. The absorption bands are due to an electron-phonon interaction of the infrared beam with the crystal lattice of the $LaAlO_3$, which is known as the restrahlen phenomenon [21]. The oscillating electric field of the infrared radiation causes a change in dipole moment in the crystal lattice, and that in turn causes absorption of vibrational energy. Each spectrum was divided by the mirror

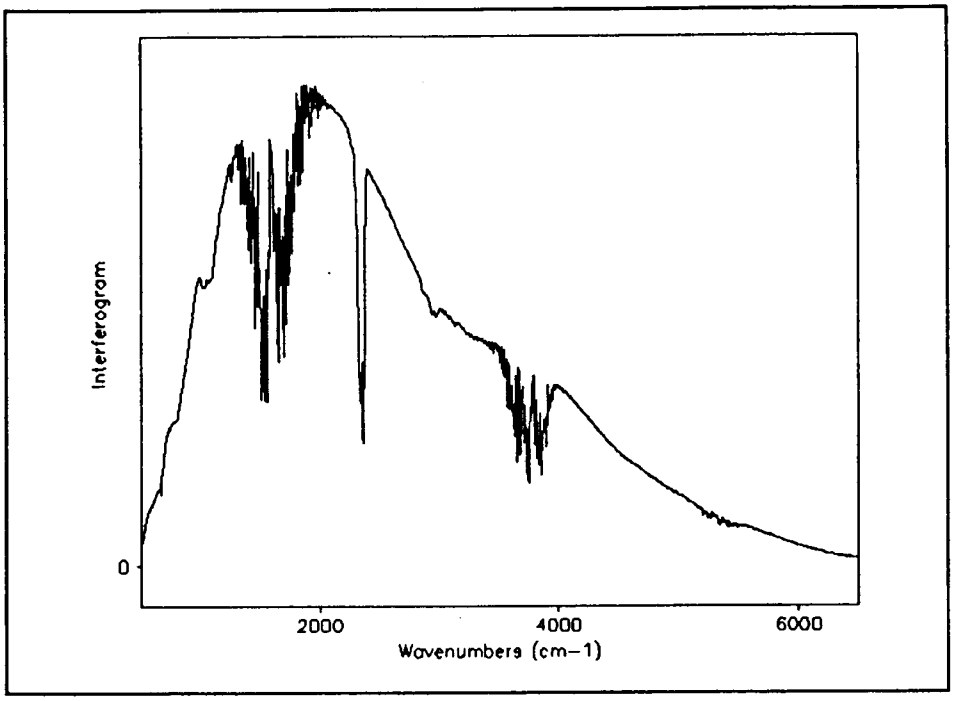

Figure 3. Mirror reference taken with the chamber *in vacuo*.

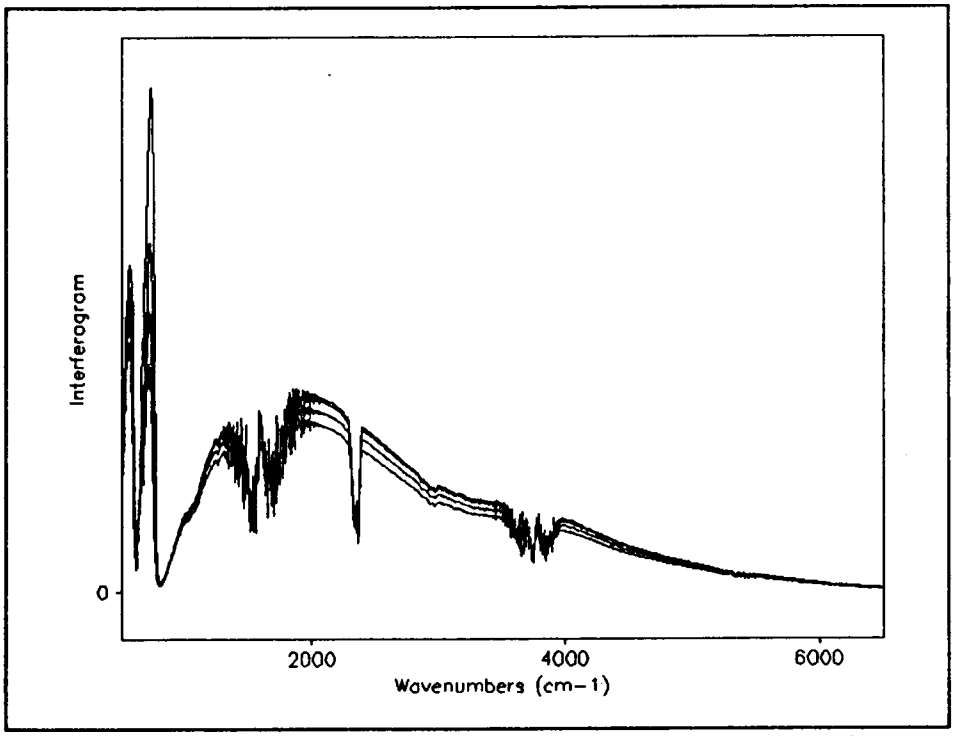

Figure 4. $LaAlO_3$ references taken before division by mirror reference.

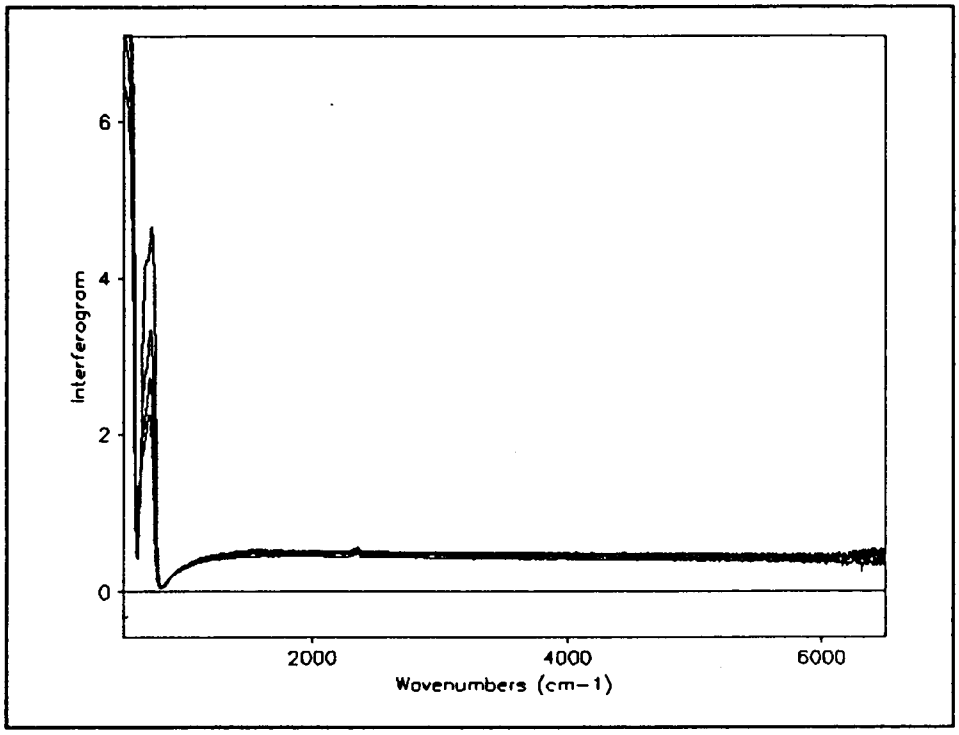

Figure 5. $LaAlO_3$ references taken after division by mirror reference.

reference to eliminate the response of the spectrometer. While the $LaAlO_3$ references were taken, there was only one screen in front of the infrared detector.

In order to deposit superconducting material on the substrate, the laser beam was directed by UV grade quartz right-angle prisms through the attenuator and into the window of the vacuum chamber, where it hit the surface of a pressed pellet of $YBa_2Cu_3O_{7-x}$ bulk superconducting material (HiTc Superconco Inc.). The motor used to rotate the target was controlled by Telix computer software. Target rotation is required because tightly focused laser radiation causes deep cratering of the target surface. That in turn causes narrow angular distribution of evaporants, power density variations, and variation of the direction of the evaporant plume [22]. The optics were adjusted so that the evaporant plume was aimed directly at the substrate, which was located 5 cm from the target.

Deposition was performed at a substrate temperature of 760 °C. FT-IR spectra were taken at regular intervals to monitor film deposition and observe phase changes in the film. An example of the changes in the FT-IR spectra are shown in Figure 6, where the reflectance versus wavenumber is shown. Each ablation decreases the relative intensity of the spectrum at low wavenumbers, and the spectrum of a good film also begins to "flatten out." Notice that the absorption bands are shifted to lower wavenumbers as the ablation process continues. Deposition times varied with laser wavelength and fluence. When deposition was completed, the chamber pressure was increased to 250 Torr O_2. This has been shown to be sufficient to produce superconducting films without the need for post-annealing in high oxygen pressures [24].

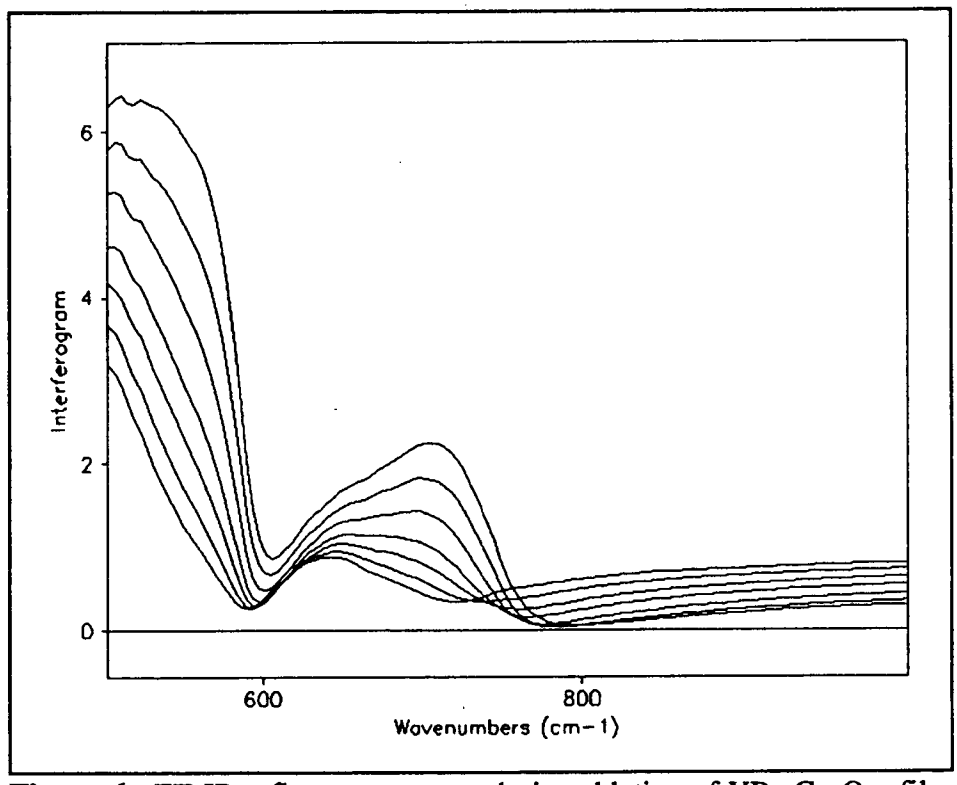

Figure 6. FT-IR reflectance spectra during ablation of $YBa_2Cu_3O_{7-x}$ film at 3 J/cm^2 fluence and 266 nm wavelength.

FT-IR spectra showed a dramatic change as oxygen was being incorporated into the film in previous experiments [24]. The addition of oxygen after deposition seems to complete the phase change from tetragonal to orthorhombic [25]. The substrate temperature was lowered to 600 °C, 400 °C, and then room temperature. Interferograms were taken at each temperature and divided by the mirror reference.

The vacuum chamber was backfilled to 1 atm with O_2 gas and the substrate was removed. The substrate was then mounted on a resistance probe, while wires were connected to the film surface with silver paint. The probe was placed in a CRYO Industries of America, Inc. Model RC 151 cryogenic workstation and four-wire resistance measurements were taken by computer for the temperature range 80 K to 120 K using liquid nitrogen. (Computer program used to record resistance versus temperature is listed in Appendix A.) In this experiment a Hewlett-Packard 3478A multimeter and a LakeShore 308 temperature controller were used.

CHAPTER 3

DEPENDENCE ON LASER FLUENCE

The experimental procedure was described in Chapter 2. For the first set of experiments, the 266 nm wavelength was used for laser ablation to study the effect of laser fluence on superconducting thin film quality. It was already known that ultraviolet light produces better films than other wavelengths due to good absorption of laser energy by the $YBa_2Cu_3O_{7-x}$ material and therefore smaller particulates in the evaporant plume [26].

For this set of experiments, it was not possible to attenuate the laser beam in order to maintain constant target area due to low laser energy (approximately 20 mJ energy at the target) and range of fluences. Therefore, the area needed for a certain laser fluence and 20 mJ energy was calculated, and then the lens was positioned to obtain the desired target area (see Appendix B for the calculation of lens position and target area). For each wavelength, the actual focal length of the lens was measured. Laser fluences of 10, 5, 3, 1, and 0.5 J/cm^2 were used, and the area varied from 0.002 cm^2 to 0.04 cm^2. Deposition time was 50 minutes for each film. The results of the FT-IR reflectance spectra and the resistance measurements are shown in Figures 7-16. The infrared reflectance spectra agree with those obtained for similar $YBa_2Cu_3O_{7-x}$ samples [27, 28]. The trace with the lowest relative intensity was taken immediately after the last

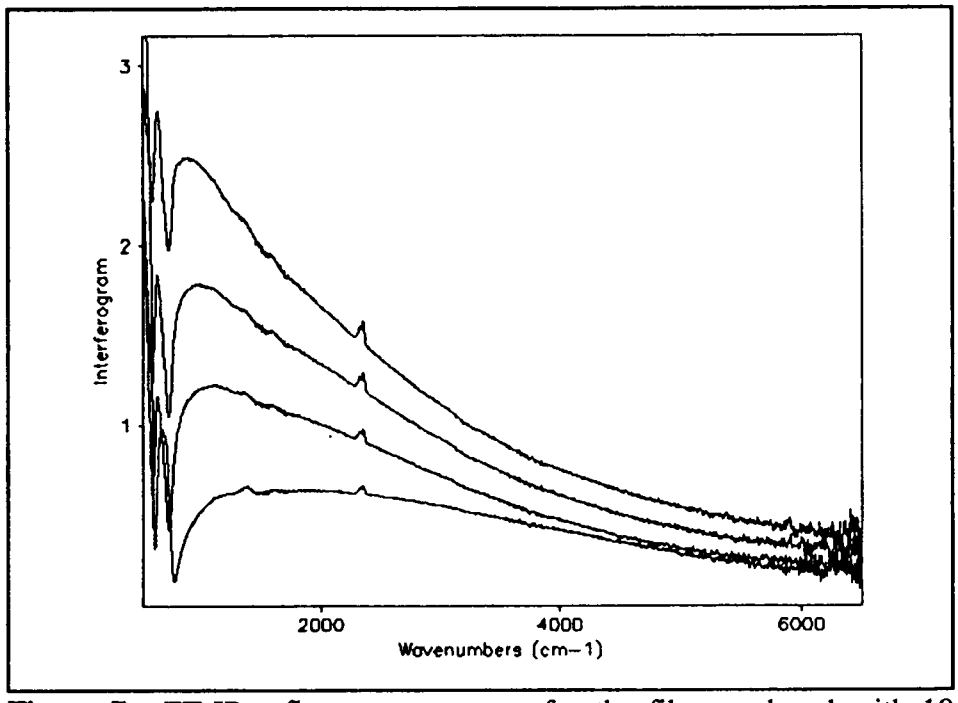

Figure 7. FT-IR reflectance spectrum for the film produced with 10 J/cm^2 fluence and 266 nm wavelength.

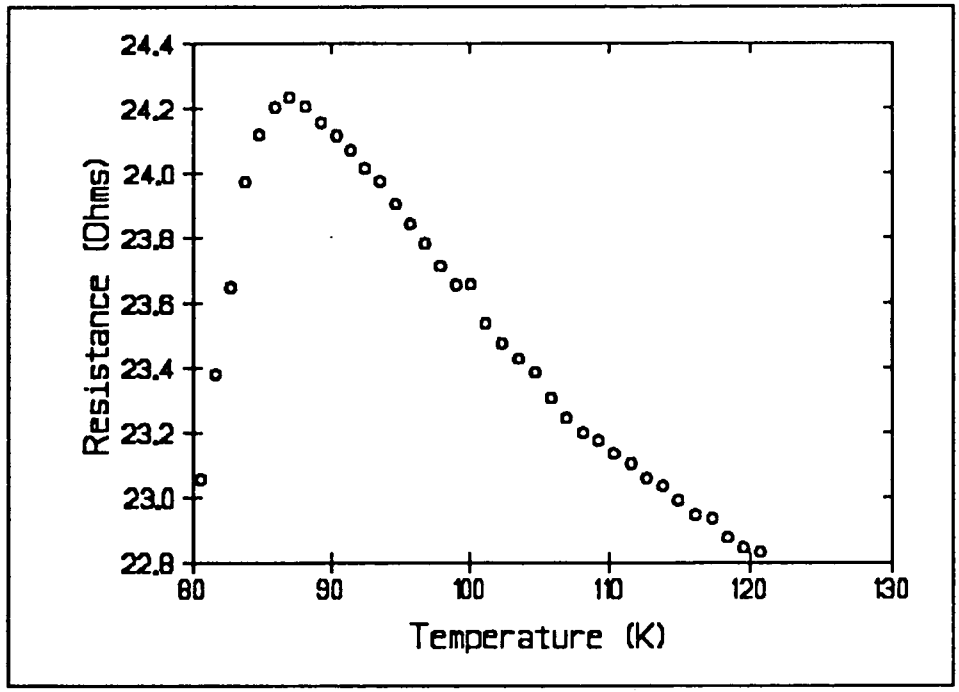

Figure 8. Resistance versus temperature for the film produced with 10 J/cm^2 fluence and 266 nm wavelength.

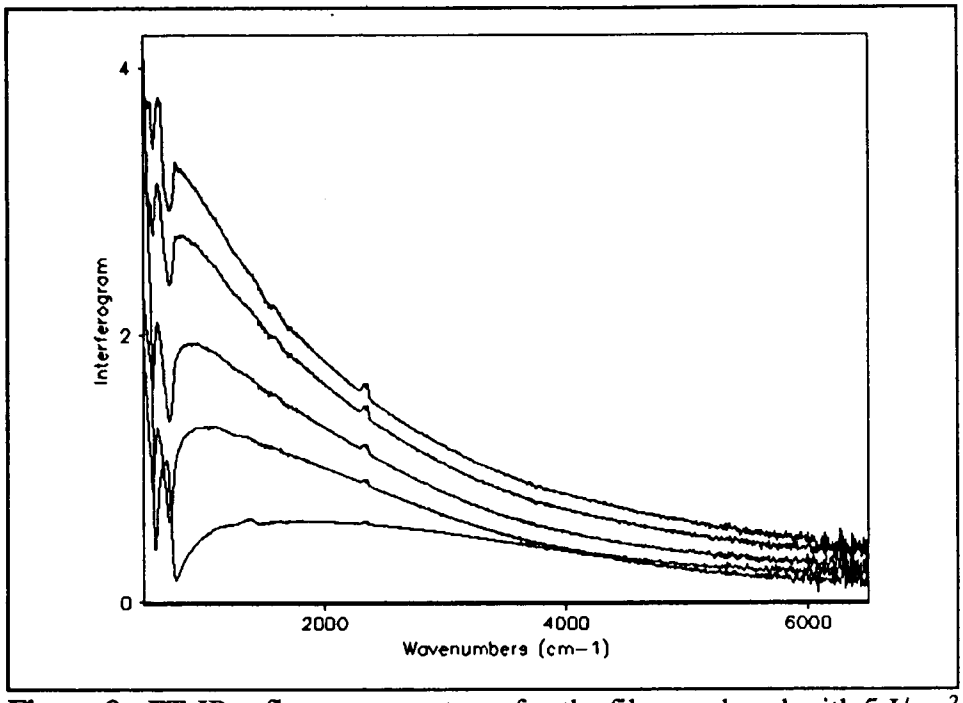

Figure 9. FT-IR reflectance spectrum for the film produced with 5 J/cm^2 fluence and 266 nm wavelength.

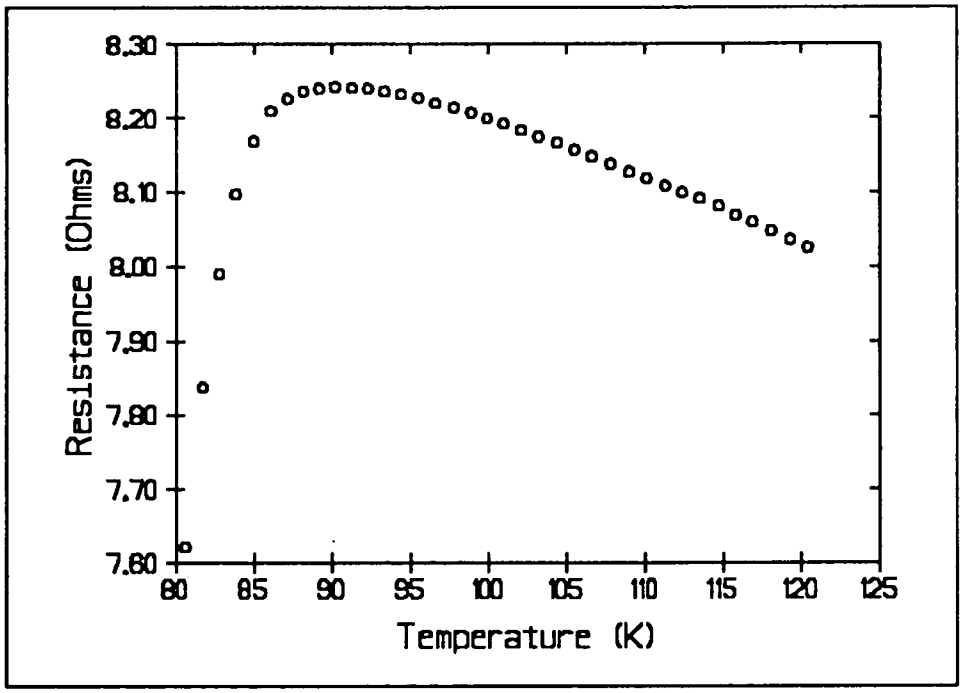

Figure 10. Resistance versus temperature for the film produced with 5 J/cm^2 fluence and 266 nm wavelength.

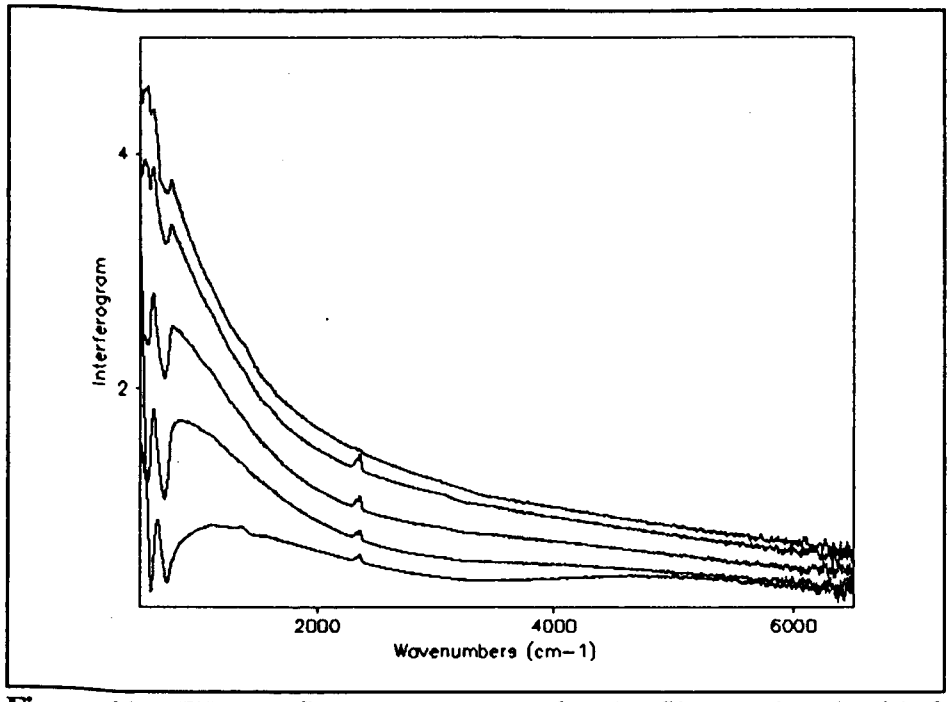

Figure 11. FT-IR reflectance spectrum for the film produced with 3 J/cm^2 fluence and 266 nm wavelength.

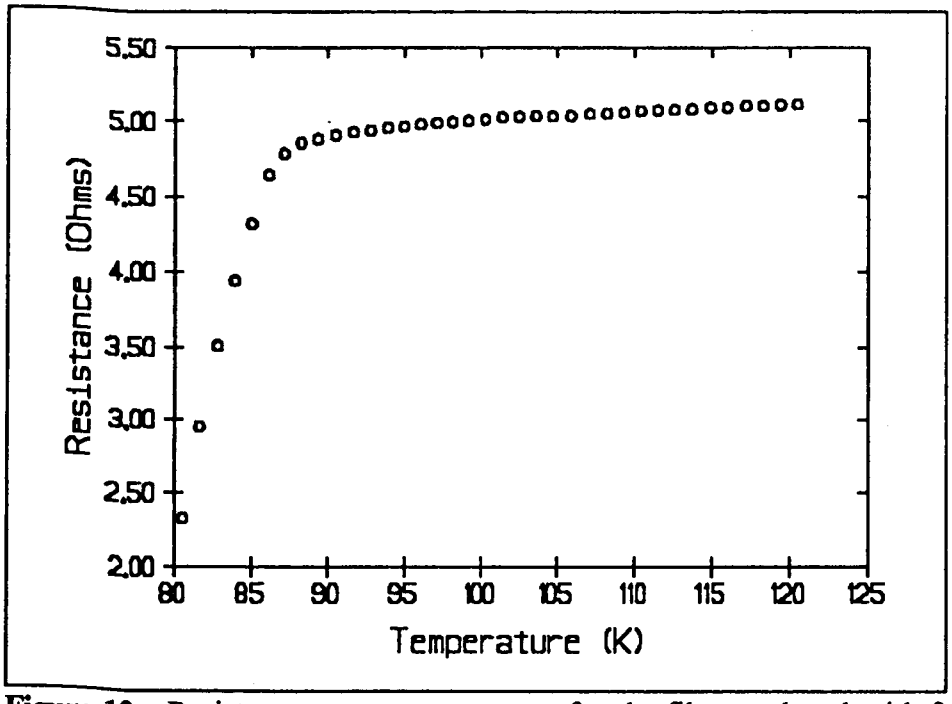

Figure 12. Resistance versus temperature for the film produced with 3 J/cm^2 fluence and 266 nm wavelength.

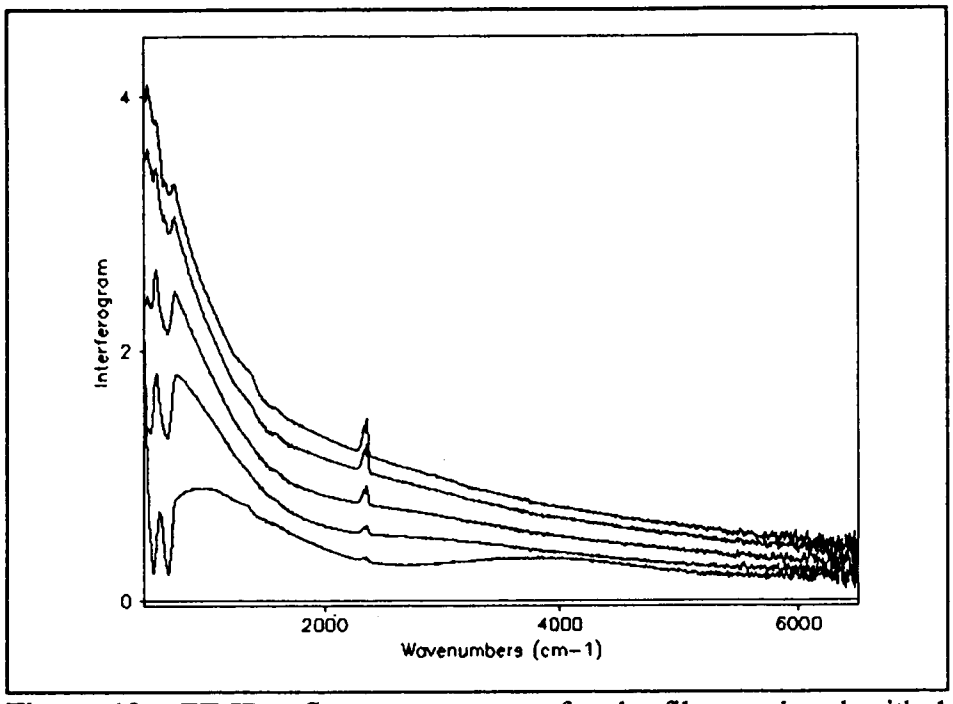

Figure 13. FT-IR reflectance spectrum for the film produced with 1 J/cm^2 fluence and 266 nm wavelength.

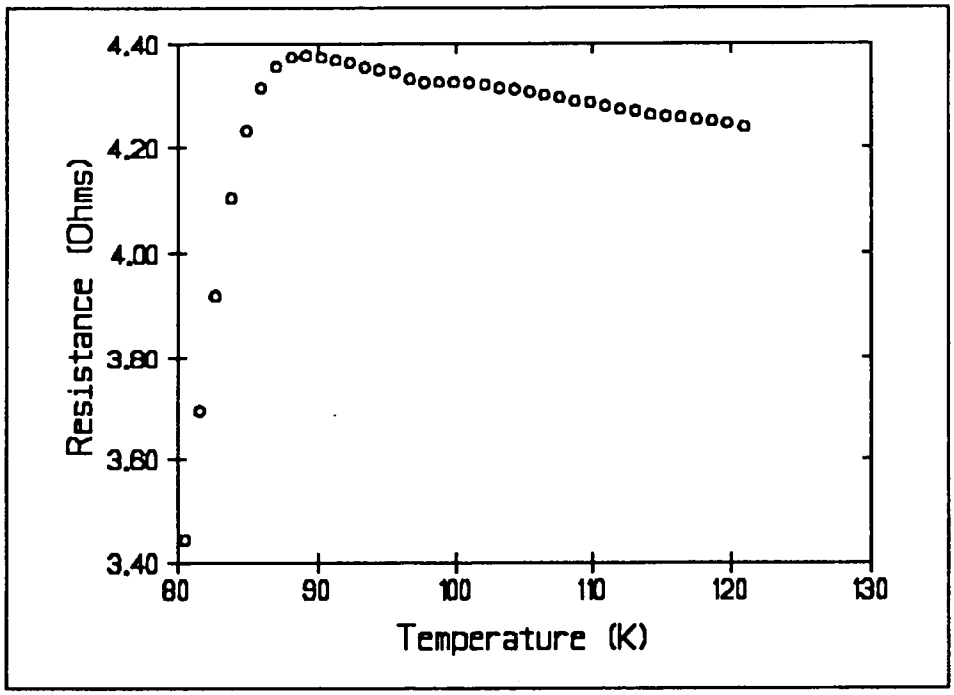

Figure 14. Resistance versus temperature for the film produced with 1 J/cm^2 fluence and 266 nm wavelength.

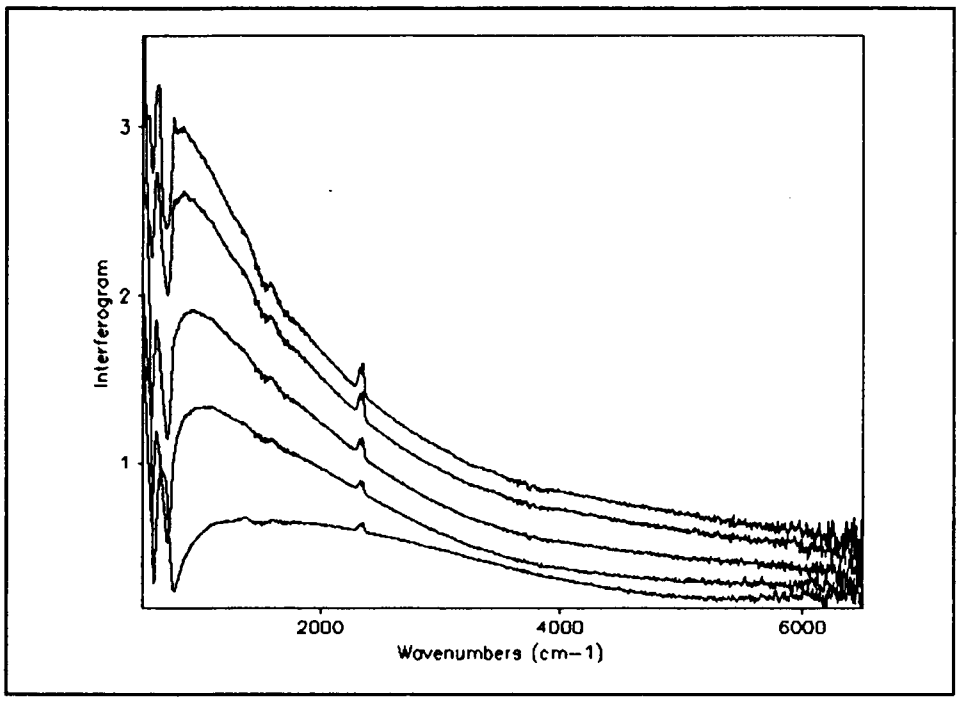

Figure 15. FT-IR reflectance spectrum for the film produced with 0.5 J/cm^2 fluence and 266 nm wavelength.

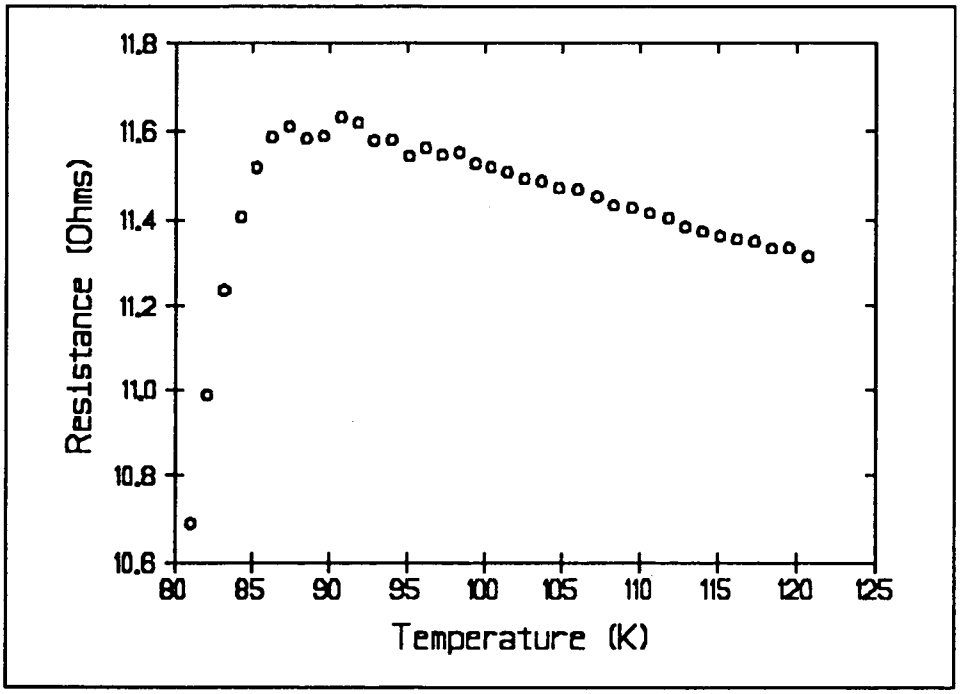

Figure 16. Resistance versus temperature for the film produced with 0.5 J/cm^2 fluence and 266 nm wavelength.

deposition. The trace with slightly higher intensity was taken after 250 Torr O_2 gas was added to the chamber, while the temperature remained at 760 °C. Traces with increasingly higher intensity correspond to 600 °C, 400 °C, and then room temperature. There is a small feature present at approximately 2500 cm^{-1} that is seen in only some of the spectra. This is probably a feature of the substrate, and since there were three different substrates used, it could mean that one or more of the substrates have more defects in their crystalline structure than the others.

A close-up of Figure 10 is shown in Figure 17. Three main absorption bands were noted at approximately 530, 590, and 710 cm^{-1} in the film at room temperature. For comparison, the $LaAlO_3$ absorption bands were seen at 610 and 800 cm^{-1}. The band at 530 cm^{-1} appeared after 250 Torr oxygen was added to the vacuum chamber. These bands are due to either the stretching of a chemical bond or the bending of an angle of a bond. External vibrational modes of crystalline substances below 800 cm^{-1} are lattice modes [29]. Another group reported absorption bands at 540-585 cm^{-1}, 590 cm^{-1}, and 620-640 cm^{-1} for fully oxygenated films, and found that the bands shifted frequency when the films were oxygen deficient [30].

In comparing the resistance versus temperature of the films, 3 J/cm^2 fluence produced the best results. This value for the fluence typically produces better quality films [24]. Note that the FT-IR spectrum at room temperature is smoother than those of the others. The absorption peaks seen at low wavenumbers have almost completely disappeared for the room temperature curve. With oxide materials, infrared absorption bands are observed to disappear when the material becomes metallic [31]. These features

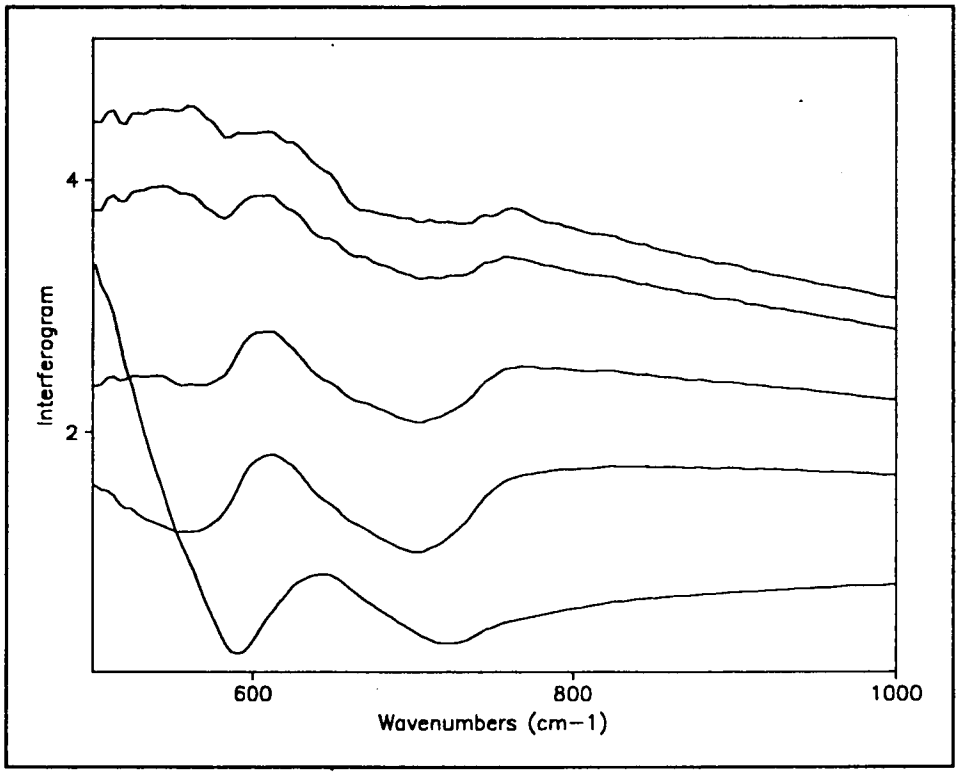

Figure 17. Close-up view of Figure 10.

are likely due to the substrate, and indeed do correspond to features seen in the $LaAlO_3$ references. If that is the case, one explanation is that a film which has strong absorption bands is not metallic and therefore highly resistive. Therefore, the infrared beam of the interferometer will probe more deeply through the film and to the substrate because of the relation between skin depth and resistivity (see Appendix C). The film produced at 3 J/cm^2 fluence has higher reflectivity and lower resistance, which means that it is more metallic than the others. The remaining films, which have more pronounced features at low wavenumbers, also have a smaller value for the slope of the curve for all wavenumbers and higher resistances. This would indicate that those films are not metallic. Therefore, the spectrum for 3 J/cm^2 fluence represents the spectrum obtained for a good metallic material, as evidenced by its reflectivity and resistance.

Even though zero resistance is not indicated on the graphs, the films show a dramatic drop in resistance as the temperature is lowered, which would indicate that they have a T_c that is below 80 K. The reason for the lower critical temperature could be explained by the films being slightly oxygen deficient, or rather, $x > 0$, causing the critical temperature to be lower than 92 K (when $x = 0$) [18]. However, annealing of a sample in oxygen at 500-550 °C for 30 minutes did not cause the transition temperature to increase. Furthermore, x-ray diffraction analysis showed additional peaks that are not seen in good quality $YBa_2Cu_3O_{7-x}$ films. The lower critical temperature of the films could also be due to impurities in the film, because the $YBa_2Cu_3O_{7-x}$ targets were not pre-ablated prior to film deposition.

CHAPTER 4

DEPENDENCE ON LASER WAVELENGTH

This set of experiments used the same conditions as described in Chapter 3, except that the area on the surface of the target was kept constant for all laser fluences. The reason for this was the fact that more energy was available at the other wavelengths.

355 nm Wavelength:

For the 355 nm wavelength, laser fluences of 20, 10, 5, 3, and 1 J/cm^2 were studied, with a target area of 0.0135 cm^2. The results for 5, 3, and 1 J/cm^2 are shown in Figures 18-23. The traces represent the same conditions used in the experiments at 266 nm. Both 3 J/cm^2 and 1 J/cm^2 fluences produced good film with low resistance and a smooth FT-IR spectrum with the absorption bands nearly gone at room temperature, but the film produced with 3 J/cm^2 fluence is slightly better. It has a sharper transition and a lower room temperature resistance, in addition to a smoother FT-IR spectrum. This film is comparable to the film produced at 266 nm wavelength. Notice that a smaller range of fluences at this wavelength produced superconducting films - 5 J/cm^2 to 1 J/cm^2 fluence. Fluences higher than 5 J/cm^2 and lower than 1 J/cm^2 produced films

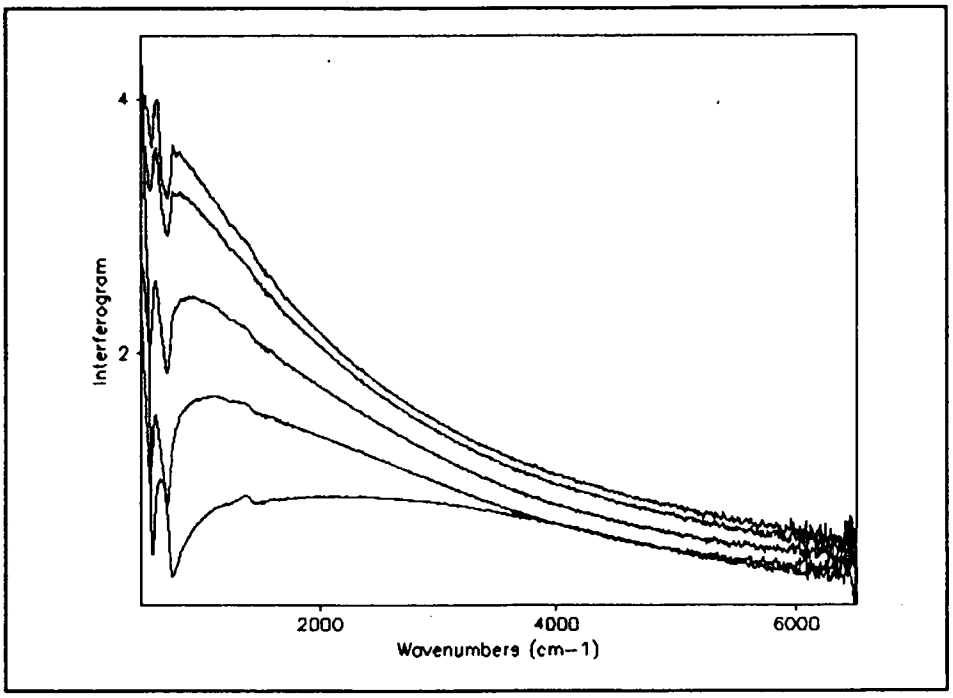

Figure 18. FT-IR reflectance spectrum for the film produced with 5 J/cm^2 fluence and 355 nm wavelength.

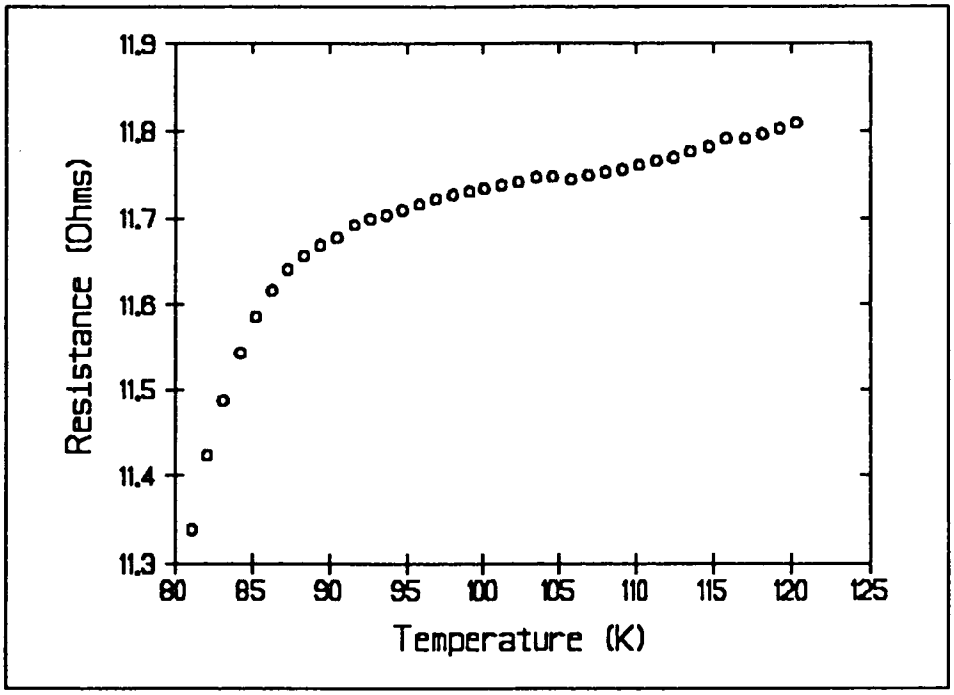

Figure 19. Resistance versus temperature for the film produced with 5 J/cm^2 fluence and 355 nm wavelength.

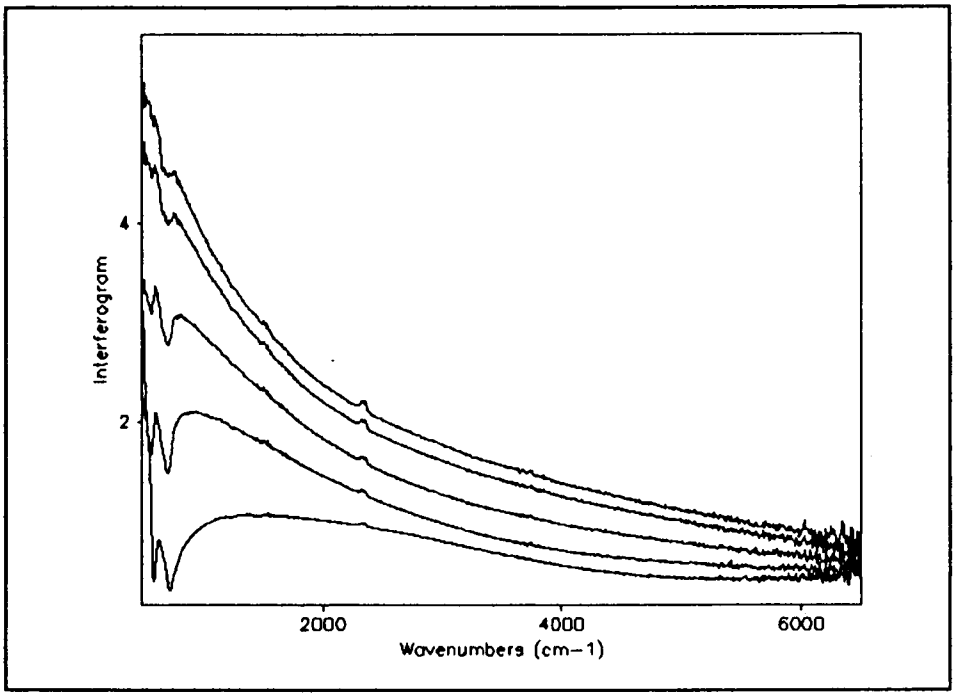

Figure 20. FT-IR reflectance spectrum for the film produced with 3 J/cm^2 fluence and 355 nm wavelength.

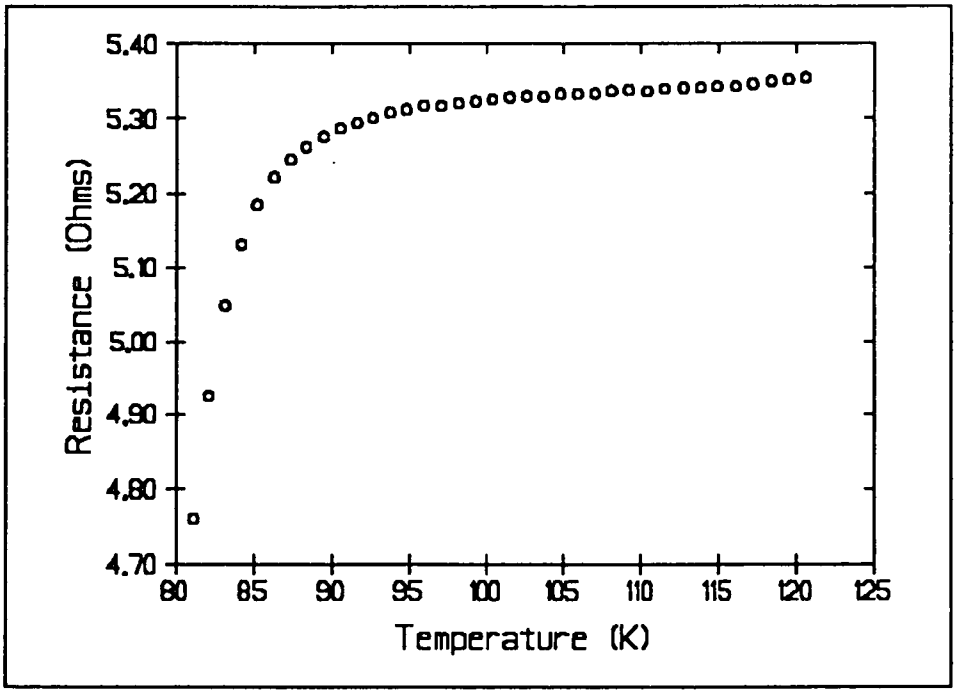

Figure 21. Resistance versus temperature for the film produced with 3 J/cm^2 fluence and 355 nm wavelength.

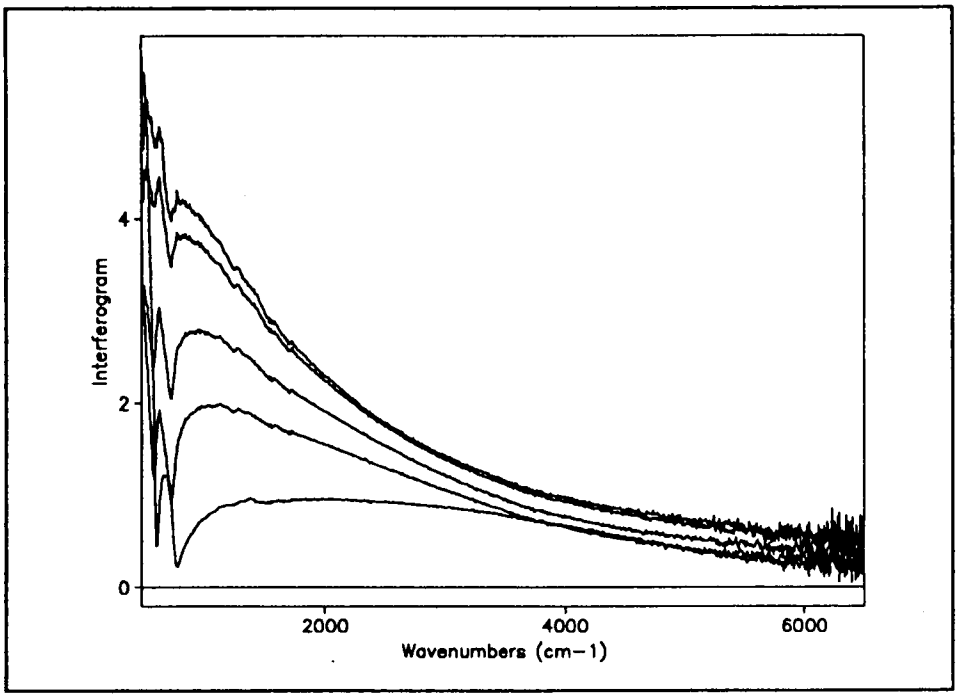

Figure 22. FT-IR reflectance spectrum for the film produced with 1 J/cm^2 fluence and 355 nm wavelength.

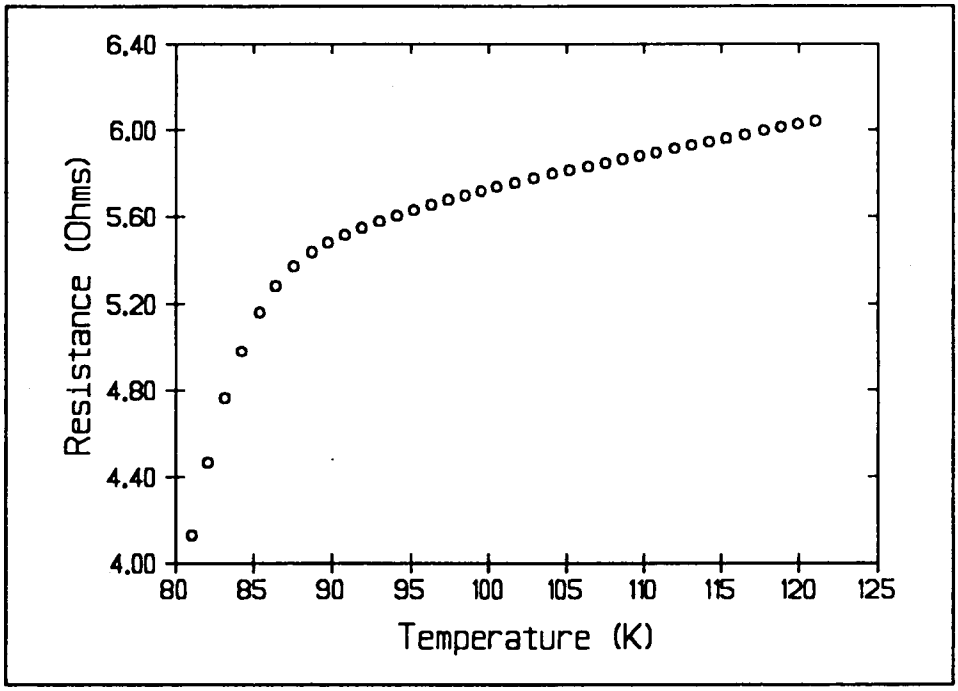

Figure 23. Resistance versus temperature for the film produced with 1 J/cm^2 fluence and 355 nm wavelength.

which had more intense absorption bands in their infrared spectra and higher values of resistance.

532 nm Wavelength:

Target area was also kept constant for the 532 nm wavelength at 0.0135 cm^2, and laser fluences of 20, 10, 5, 3, and 1 J/cm^2 were studied. The data obtained for 5, 3, and 1 J/cm^2 are shown in Figures 24-29. Notice that only 3 J/cm^2 fluence produced a film with a superconducting transition. This is presumably due to larger particulates being produced during ablation, which is discussed further in the next section. Higher fluences than 5 J/cm^2 and lower fluences than 1 J/cm^2 produced films which had stronger infrared absorption bands and higher values of resistance. One factor that was different than the results for the 355 nm wavelength was that the plume size for 532 nm wavelength was much larger, even though the target area was the same. A fluence of 5 J/cm^2 caused the evaporant plume to reach the substrate.

1060 nm Wavelength:

As in the case of 355 nm and 532 nm wavelengths, the target area was kept constant for all laser fluences. For this set of experiments, 10, 5, 3, 1, and 0.5 J/cm^2 laser fluences were used, with a target area of 0.0280 cm^2. Results obtained for 5, 3, and 1 J/cm^2 are shown in Figures 30-35. Fluences higher than 5 J/cm^2 and lower than 1 J/cm^2 produced films with more pronounced infrared absorption bands and higher values of resistance. Plume size was much larger than any other wavelength and

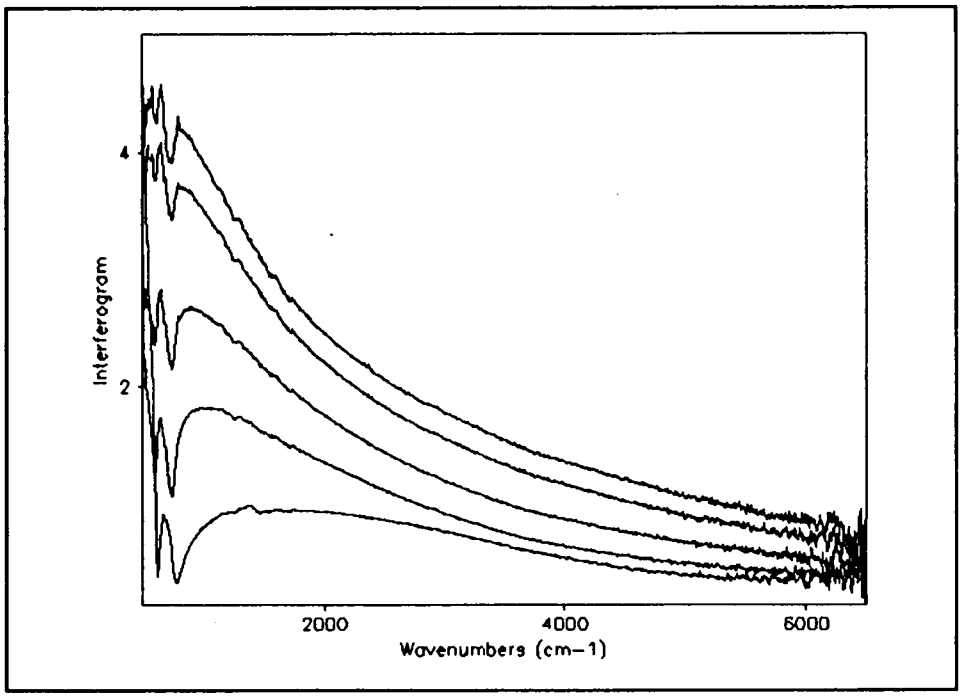

Figure 24. FT-IR reflectance spectrum for the film produced with 5 J/cm^2 fluence and 532 nm wavelength.

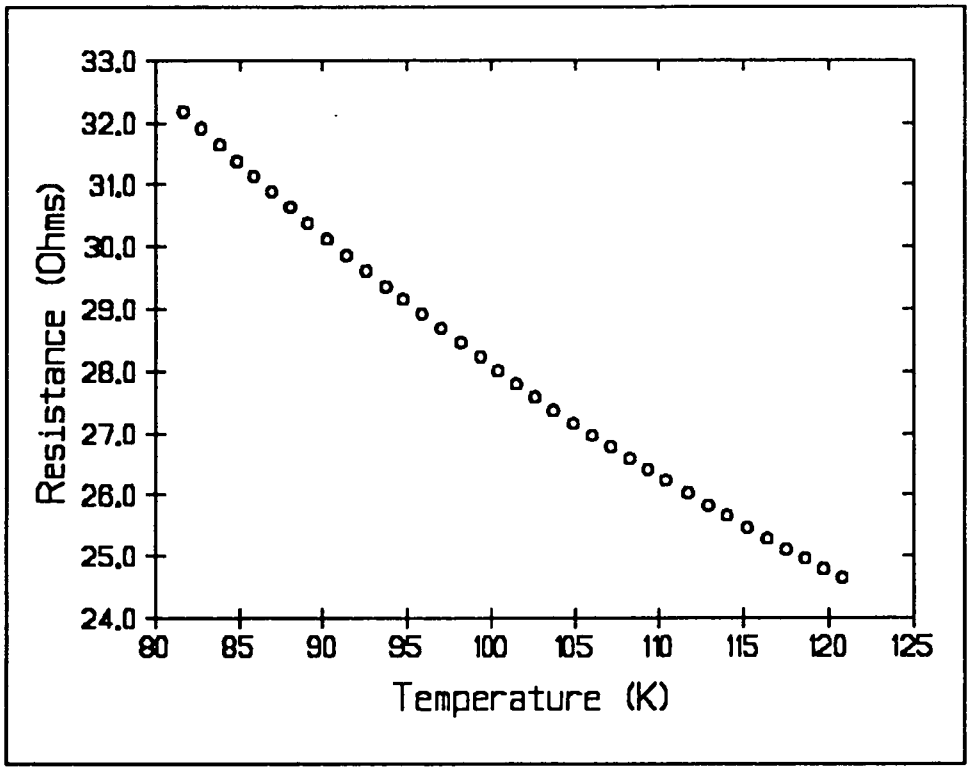

Figure 25. Resistance versus temperature for the film produced with 5 J/cm^2 fluence and 532 nm wavelength.

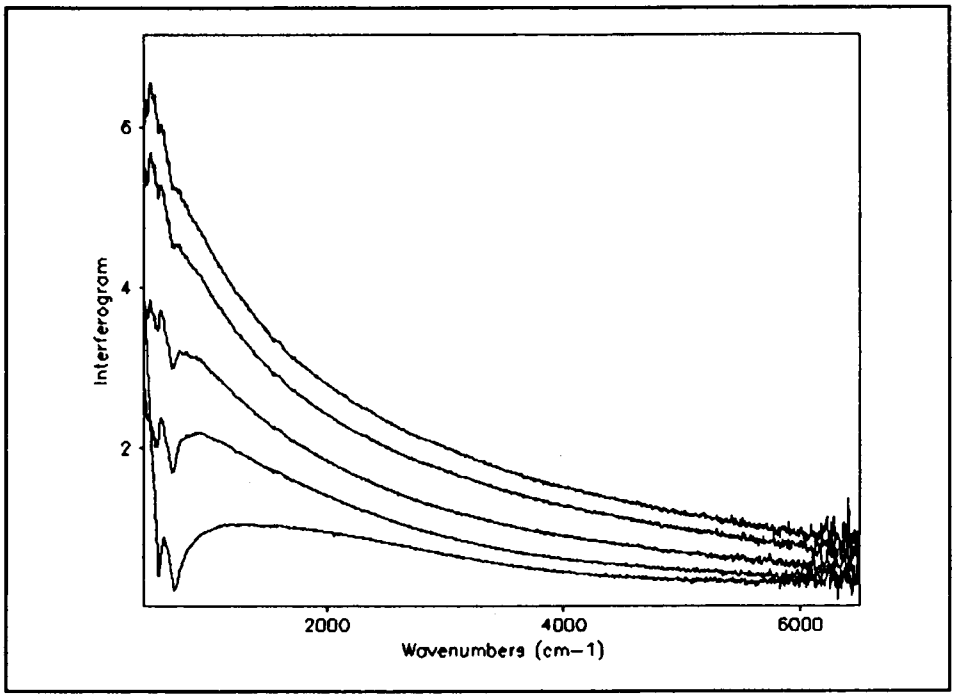

Figure 26. FT-IR reflectance spectrum for the film produced with 3 J/cm^2 fluence and 532 nm wavelength.

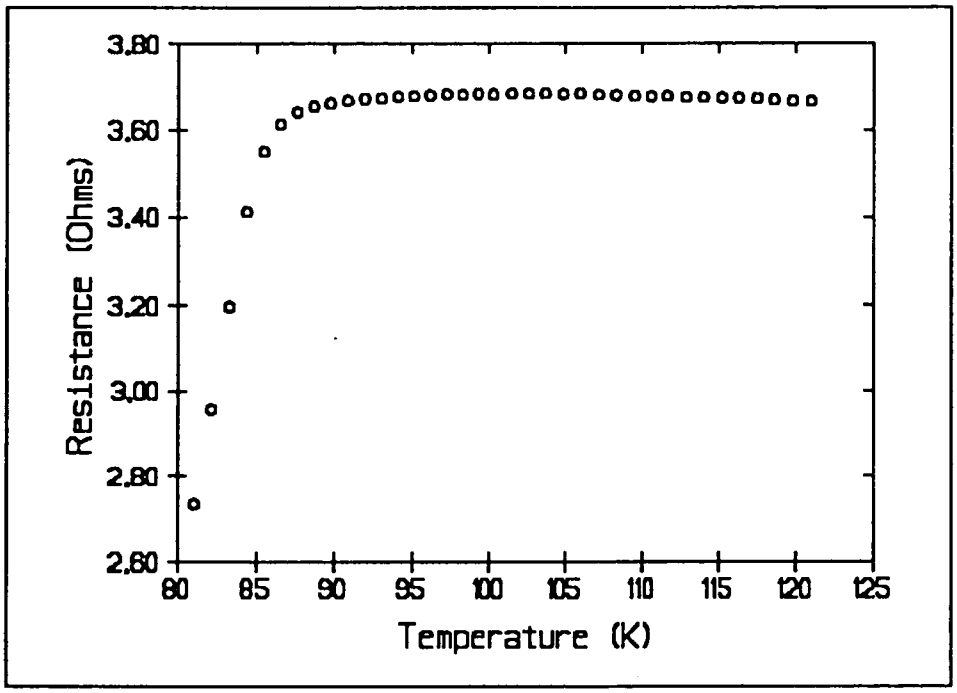

Figure 27. Resistance versus temperature for the film produced with 3 J/cm^2 fluence and 532 nm wavelength.

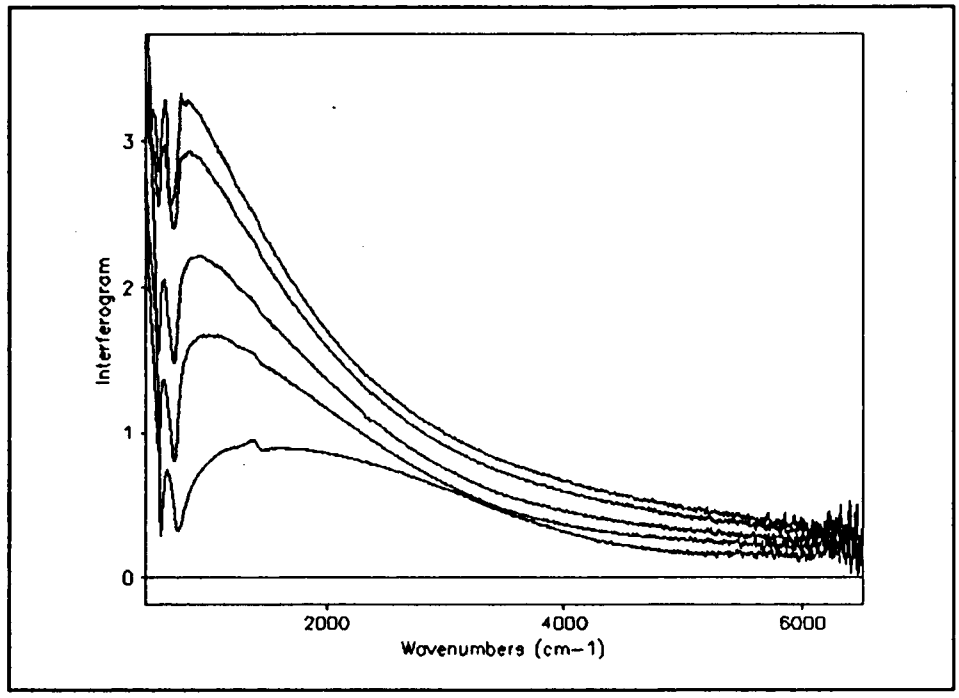

Figure 28. FT-IR reflectance spectrum for the film produced with 1 J/cm^2 fluence and 532 nm wavelength.

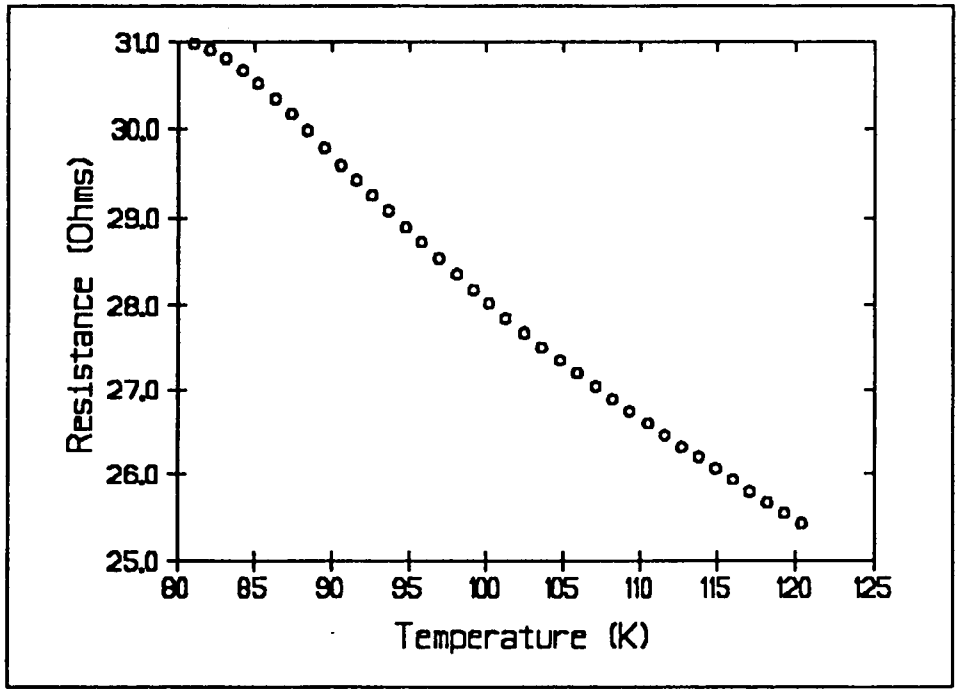

Figure 29. Resistance versus temperature for the film produced with 1 J/cm^2 fluence and 532 nm wavelength.

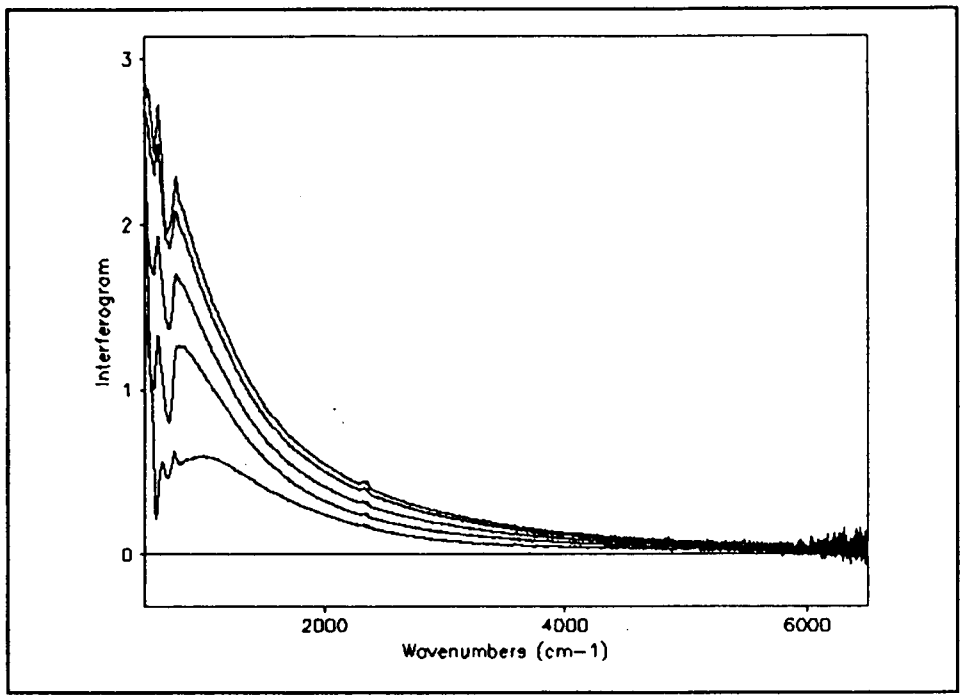

Figure 30. FT-IR reflectance spectrum for the film produced with 5 J/cm^2 fluence and 1060 nm wavelength.

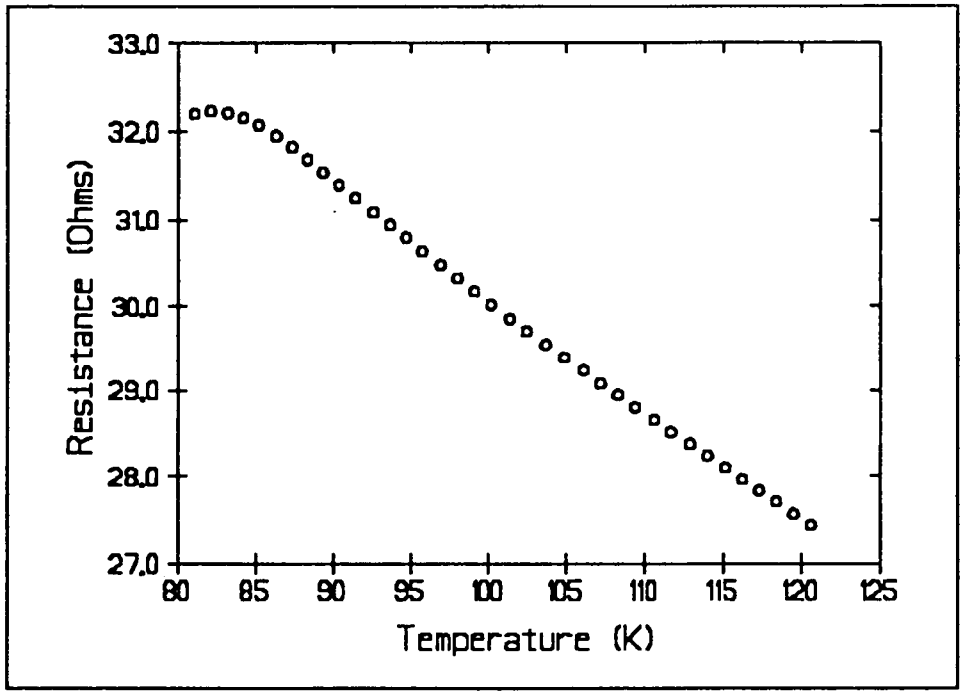

Figure 31. Resistance versus temperature for the film produced with 5 J/cm^2 fluence and 1060 nm wavelength.

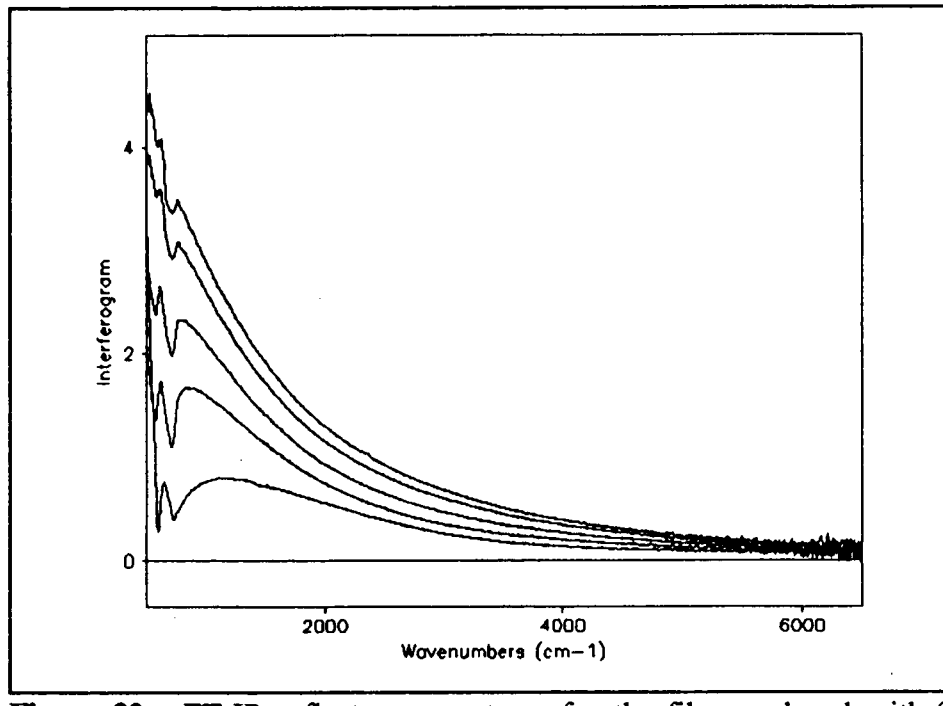

Figure 32. FT-IR reflectance spectrum for the film produced with 3 J/cm^2 fluence and 1060 nm wavelength.

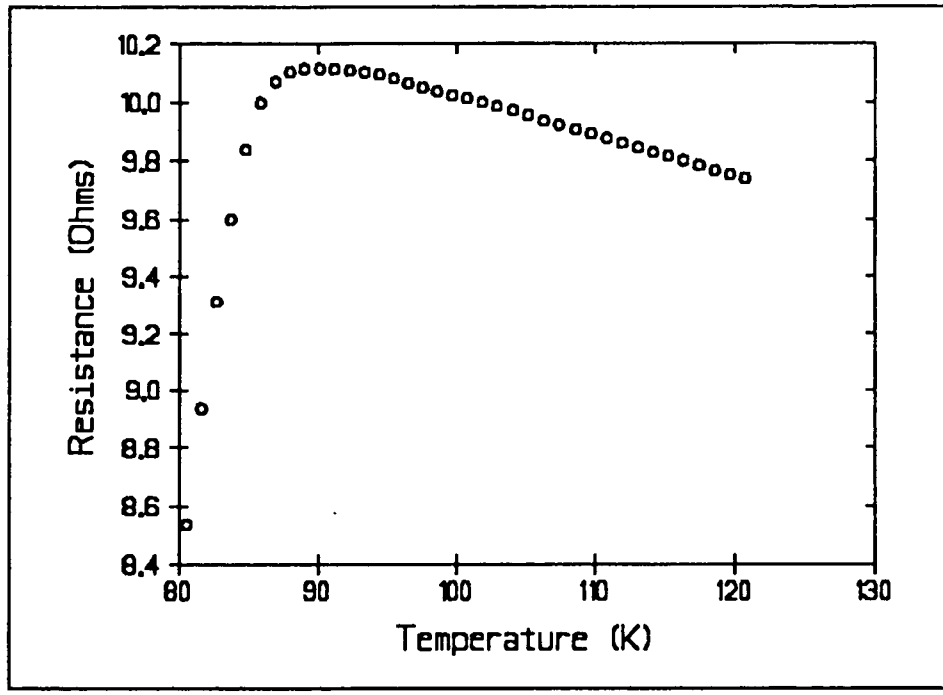

Figure 33. Resistance versus temperature for the film produced with 3 J/cm^2 fluence and 1060 nm wavelength.

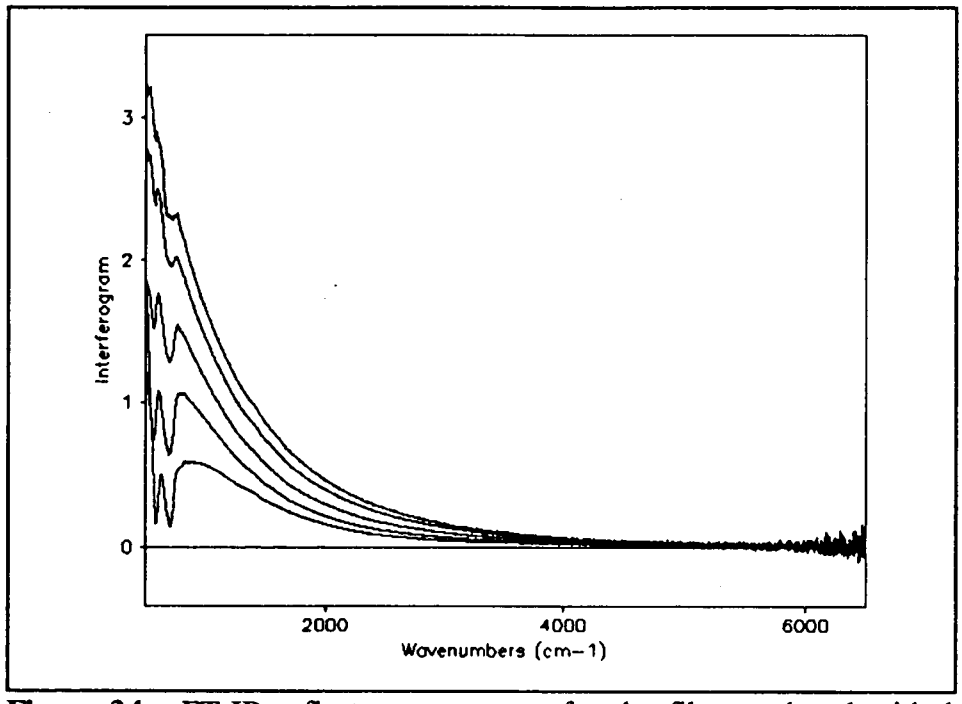

Figure 34. FT-IR reflectance spectrum for the film produced with 1 J/cm^2 fluence and 1060 nm wavelength.

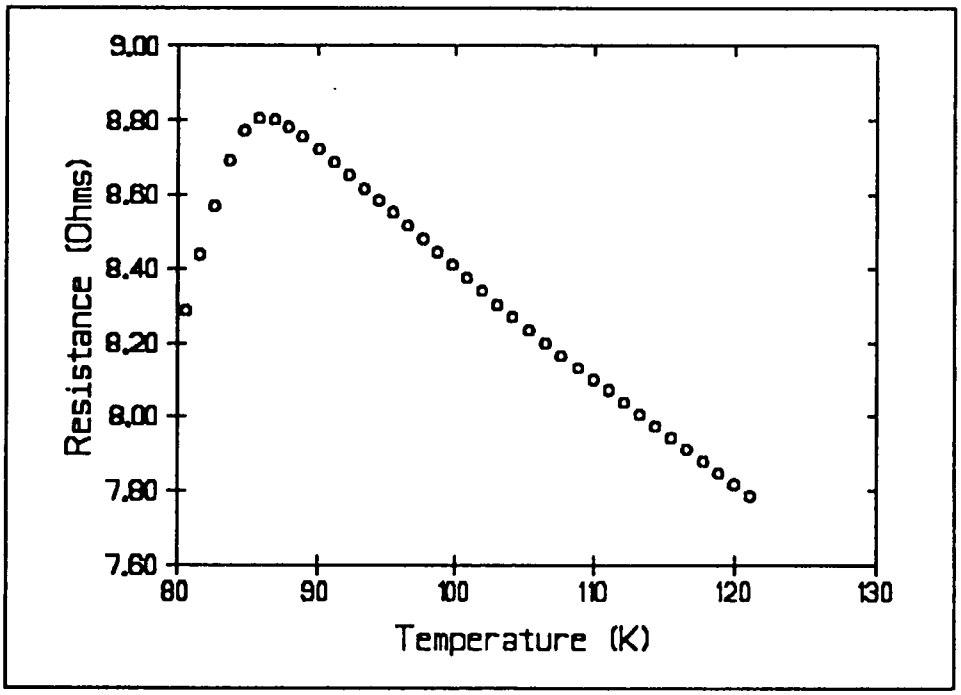

Figure 35. Resistance versus temperature for the film produced with 1 J/cm^2 fluence and 1060 nm wavelength.

deposition times were much shorter, most likely due to increased laser energy and larger target area. For higher fluences (5 or 10 J/cm^2), the evaporant plume reached the substrate.

Compared to the films produced at other wavelengths, the films produced with 1060 nm wavelength had higher values of resistance, and similar to the 532 nm wavelength, only one fluence, 3 J/cm^2, seemed to produce a film with a superconducting transition. The other fluences at 1060 nm demonstrate semiconducting behavior, which indicates a lower oxygen content. An example of the effect of oxygen content on resistivity is shown in Figure 36 [32]. This would indicate that the film which demonstrates semiconducting behavior consists of the tetragonal phase instead of the orthorhombic phase [33]. The higher laser energy causes an increase in deposition rate, but studies have shown that rates as high as 145 Å/sec produce good quality superconducting films [23]. The reason for the increased resistance is most likely due to the fact that the infrared laser radiation produces larger particulates and causes the superconducting thin film to be more inhomogeneous. Scanning electron microscopy has revealed that surface roughness increases with increasing laser wavelength [34]. Nevertheless, there appears to be enough superconducting material present to generate a critical temperature [35].

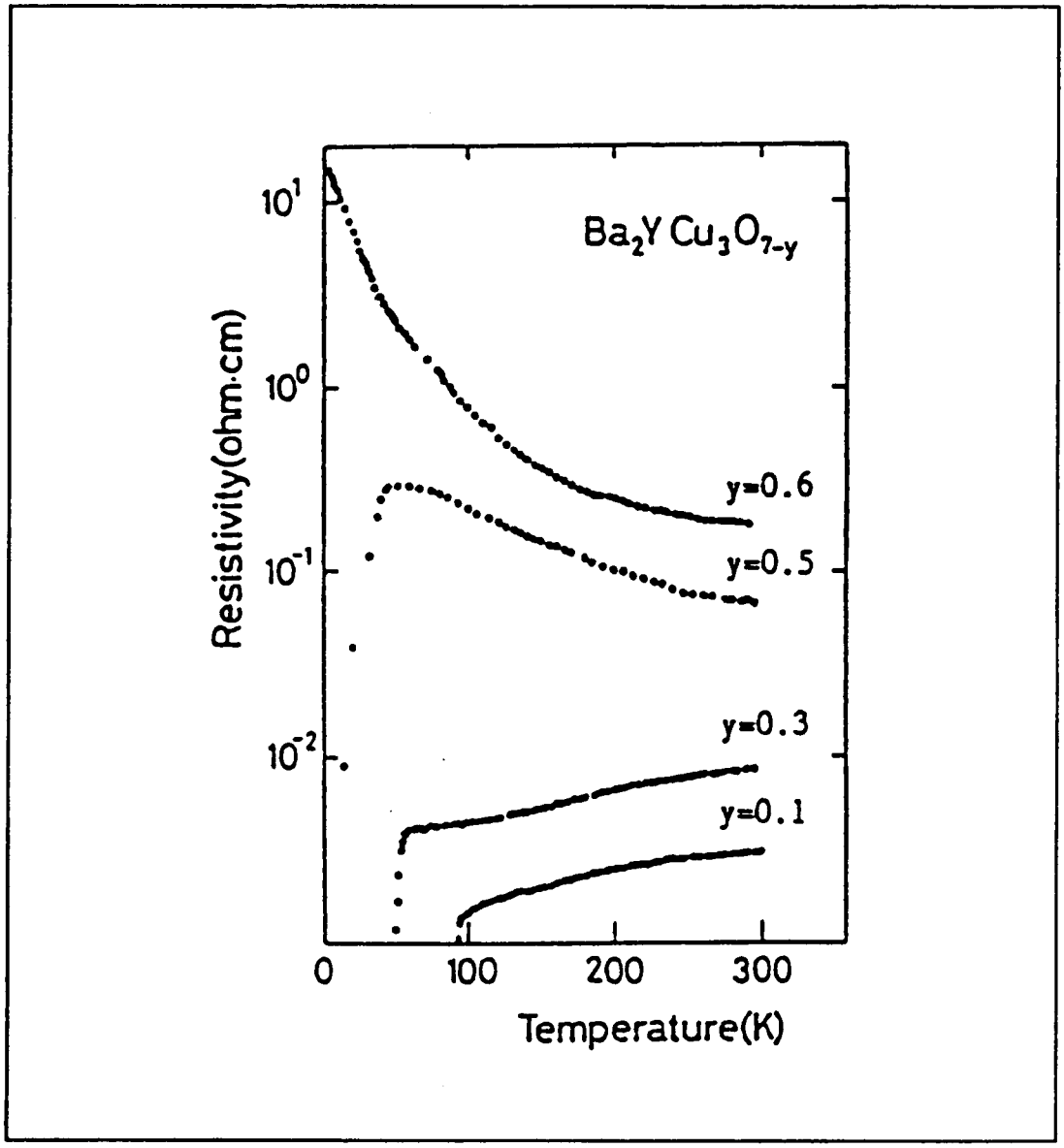

Figure 36. Effect of oxygen content on the resistivity of $YBa_2Cu_3O_{7-x}$.

Source: S. Tanaka, *et al.*, "Physical Properties and Superconductivity of Layered Perovskite Oxides," High Temperature Superconductors: Progress in High Temperature Superconductivity - vol. 1, edited by S. Lundqvist, E. Tosatti, M.P. Tosi, and Yu Lu, World Scientific, New Jersey, pp. 120-121 (1987).

CHAPTER 5

MASS SPECTRA OF ABLATED POSITIVE IONS

Laser-solid interactions depend on several factors: power density, pulse duration, wavelength, and the thermodynamic and optical properties of the target. For high power density, a high temperature plasma is produced. As laser radiation continues to strike the target, the plasma is heated and expands, partially shielding the target from further heating. As the plasma expands, it becomes transparent and allows the laser radiation to strike the target and create another plasma cloud, and the cycle continues. During laser ablation, neutral particles, electronically excited species, electrons, photons, and macroscopic particles are produced. Since the thermal cycle of heating and cooling for pulsed laser radiation is very short (in this case, a few nanoseconds), all components can be evaporated stoichiometrically [22].

An analysis of the dependence of laser wavelength and laser fluence on ablated positive ions was performed by quadrupole mass spectrometer (Extranuclear Instruments, Inc.). Originally, it was hoped that this analysis could be performed during film deposition by using a pulsed source of molecular oxygen instead of a static background O_2 pressure. Previous research showed that oxygen produced superconducting films only when it was in the vicinity of the substrate between 4 and 9 μs after the laser pulse, when the ablated fragments arrived [36]. In this particular experiment, the pulsed valve

was timed so that oxygen was delivered 200 to 400 μs after the laser oscillator, with the Q-switch operating 250 μs after the oscillator. Experiments showed, however, that operation of the pulsed valve with a chamber pressure below 1 x 10^{-4} Torr (the limitation of the mass spectrometer) resulted in films that were not superconducting at 3 J/cm^2 fluence and 266 nm laser wavelength, the optimum deposition conditions. Evidentally, the pulsed valve did not deliver enough oxygen to complete incorporation into the films.

Because of the problems with the pulsed valve, the mass spectrometer analysis was performed independently of the film deposition. First, the data were taken with the chamber under vacuum. Later, data were taken with the pulsed valve operating with an oxygen inlet pressure of approximately 45 psi, with a chamber pressure of 8.3 x 10^{-5} Torr. This hopefully would simulate the 200 mTorr background O_2 pressure and at the same time, allow the operation of the mass spectrometer to analyze the ablated material. The same wavelengths and fluences that were used to produce the films were duplicated for this experiment.

For both experiments, the signal from the channeltron was sent through a pre-amp and then an amplifier before it was read from an oscilloscope. The oscilloscope was triggered externally by the Nd:YAG laser. A typical mass spectrum in shown in Figure 37. The results from both experiments are summarized in the following:

1) For all wavelengths and fluences, more Ba^+ ions were produced than Y^+ or Cu^+ ions; explicitly, stoichiometry was not reproduced by the ablated positive ions.

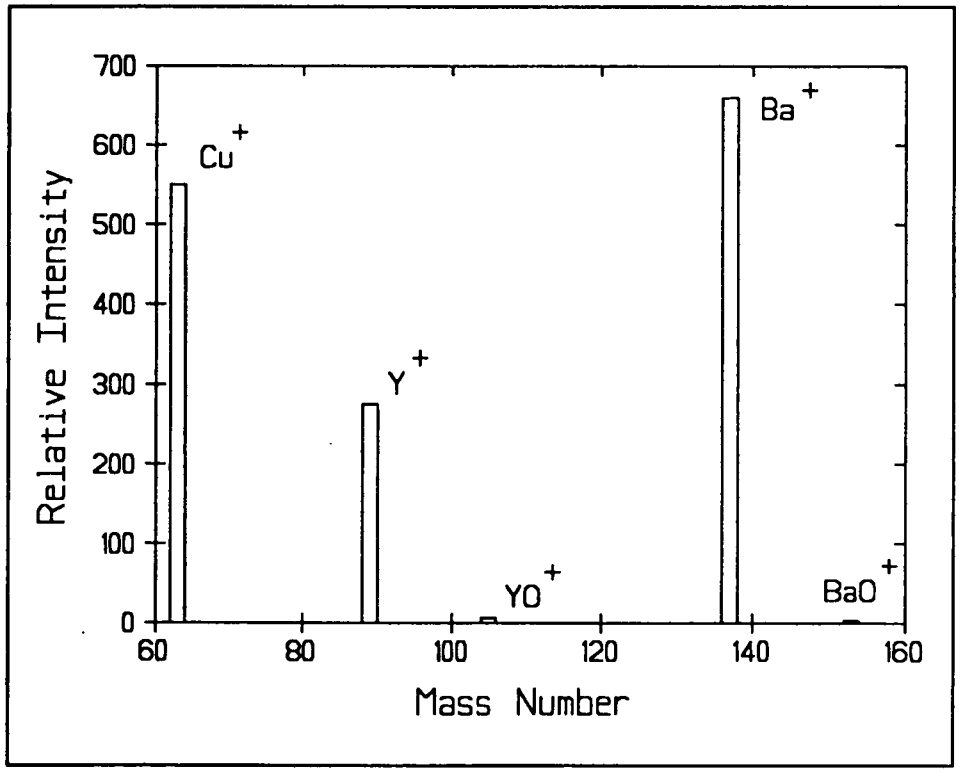

Figure 37. Typical mass spectra obtained from experiment.

2) At low fluences, it was much easier to produce Ba^+ ions than Y^+ ions, while Cu^+ ions became more difficult to detect.

3) No CuO^+ ions were detected, a finding similar to other groups [37].

4) Higher fluences produced fewer oxide ions, probably due to dissociation of O_2. Molecular oxygen is required to produce oxide ions:

$$Cu + O_2 \rightarrow CuO + O$$

Subsequent absorption by photons dissociated existing oxide ions.

$$CuO \xrightarrow{h\nu} Cu + O$$

5) Shorter wavelengths produced fewer oxide ions, probably due to the fact the photon absorption is stronger for shorter wavelengths than longer wavelengths.

6) Operation of pulsed valve caused the number of oxide ions to increase.

One theory that might explain these results is that the predominant evaporants produced during laser ablation are large clusters of material, which are not detectable by conventional mass spectrometers. It was previously assumed that ions and neutral particles were the main particulates produced. Photon absorption breaks up the clusters depending on laser wavelength. This would explain why stoichiometry is preserved in films produced by the same method as described here, while it is not preserved by the ablated positive ions [6]. Since clusters of the target material would be deposited directly on the substrate, the film would consist of $YBa_2Cu_3O_{7-x}$.

CHAPTER 6

SEM PHOTOGRAPHS OF SELECTED FILMS

The effect of laser wavelength and fluence on film particle size was studied by scanning electron microscope (SEM). A film was prepared at 3 J/cm^2 fluence for each wavelength: 266 nm, 355 nm, 532 nm, and 1060 nm. SEM photographs of these films are shown in Figures 38-45. As expected, the films produced at shorter wavelengths (266 nm and 355 nm) were smoother and had smaller particles in addition to more uniform particle size. Films produced with 532 nm and 1060 nm wavelengths had many large particles and a rougher texture, with 1060 nm wavelength producing the worst results. These findings are consistent with reports of similar experiments by other researchers [23, 26]. As stated previously, longer wavelengths are not absorbed by the $YBa_2Cu_3O_{7-x}$ target as well as shorter wavelengths, and cause a more violent expulsion of evaporants. Subsequent photon absorption by the ablated material is not as strong for longer wavelengths as for shorter wavelengths, so the clusters are not broken up into smaller pieces.

Additional films were prepared with 355 nm laser wavelength and 1, 10, and 20 J/cm^2 fluences. These films are shown in Figures 46-51. It is interesting to note that higher fluences produced larger particles. It has been suggested that higher fluences

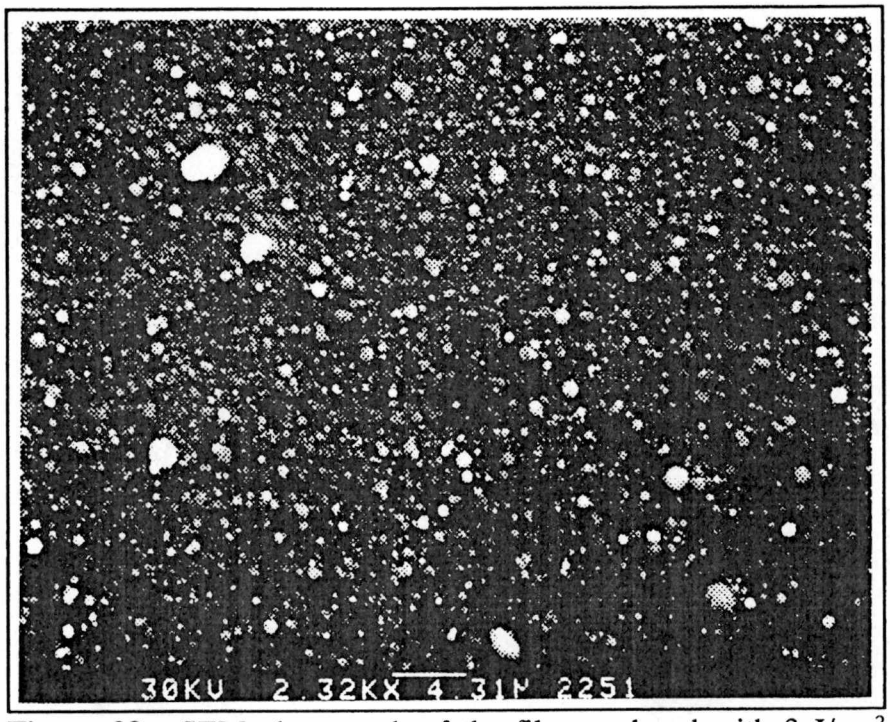

Figure 38. SEM photograph of the film produced with 3 J/cm^2 fluence and 266 nm wavelength.

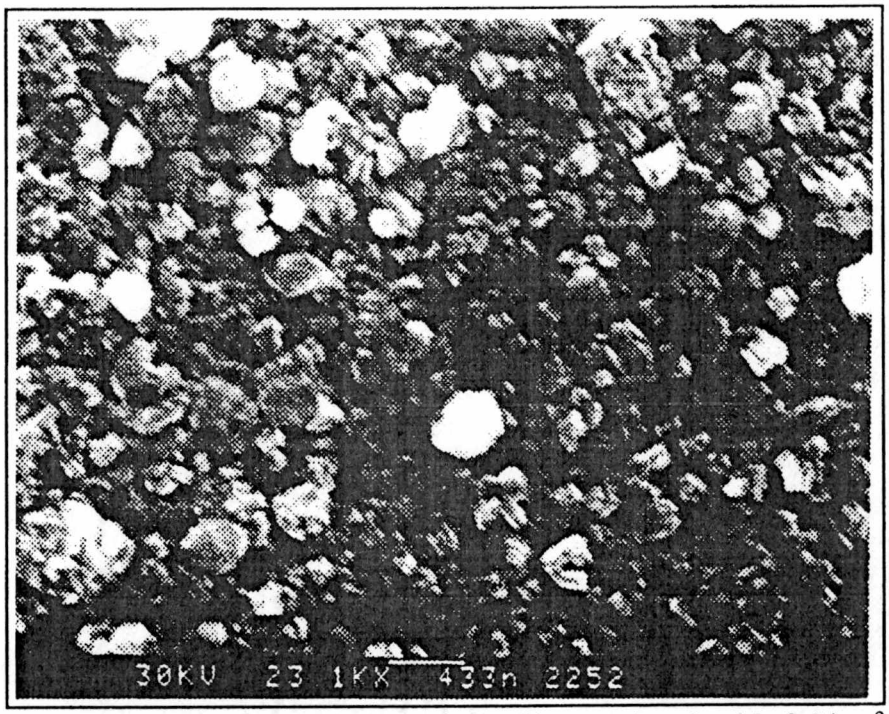

Figure 39. SEM photograph of the film produced with 3 J/cm^2 fluence and 266 nm wavelength.

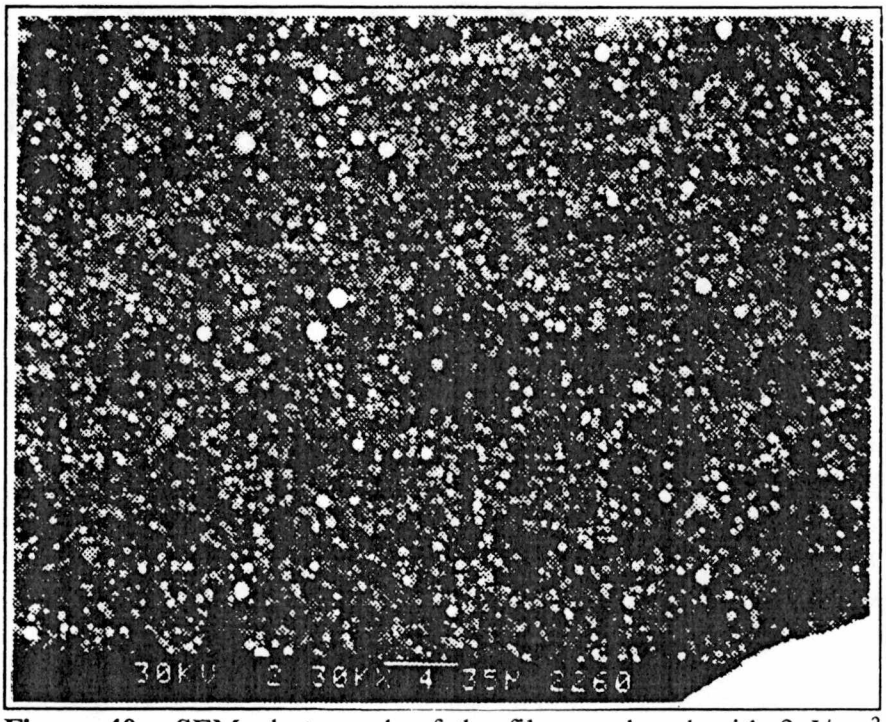

Figure 40. SEM photograph of the film produced with 3 J/cm^2 fluence and 355 nm wavelength.

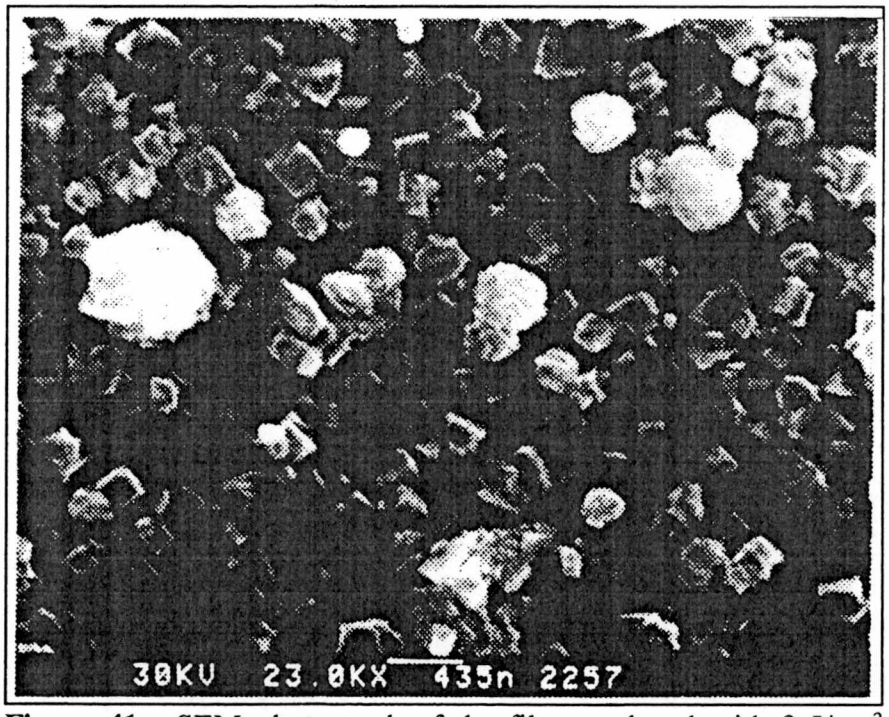

Figure 41. SEM photograph of the film produced with 3 J/cm^2 fluence and 355 nm wavelength.

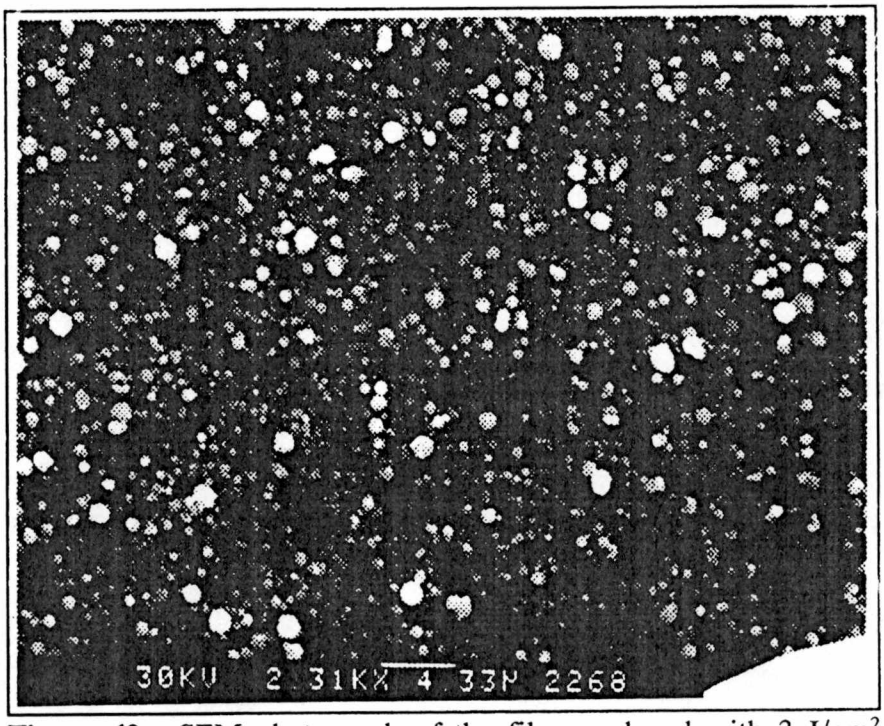

Figure 42. SEM photograph of the film produced with 3 J/cm^2 fluence and 532 nm wavelength.

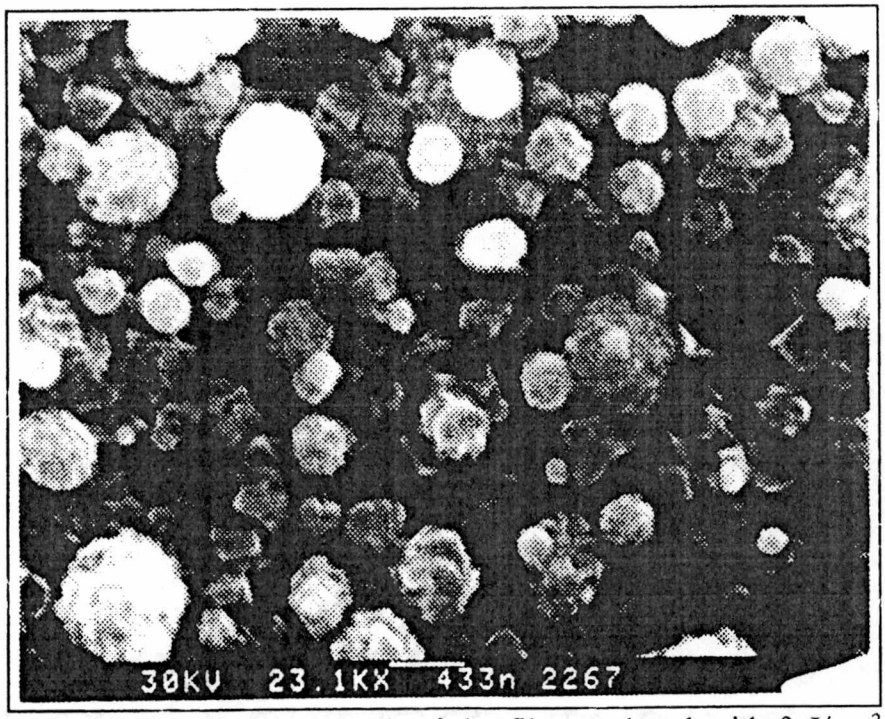

Figure 43. SEM photograph of the film produced with 3 J/cm^2 fluence and 532 nm wavelength.

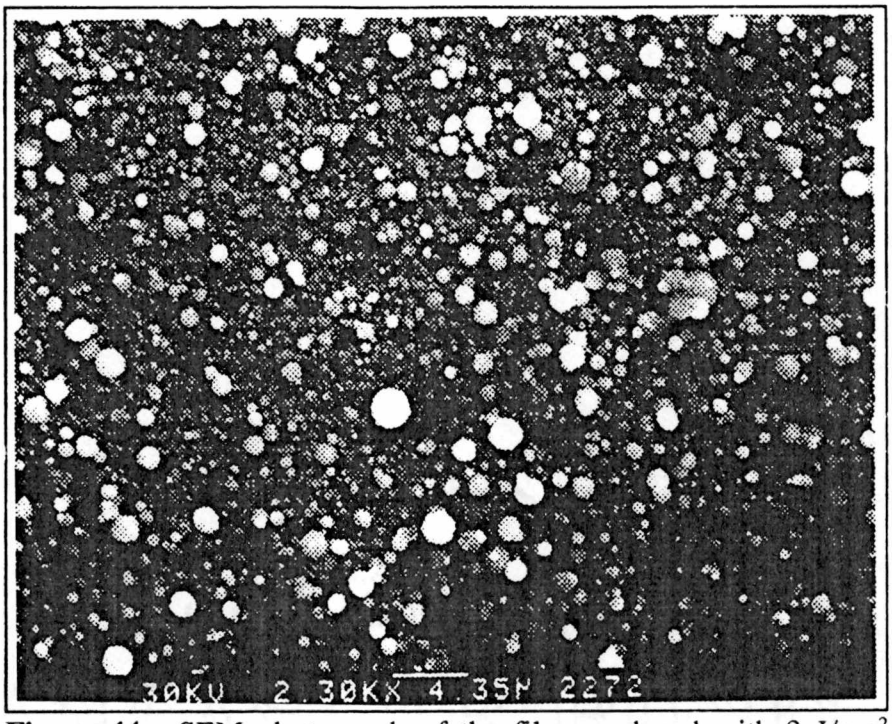

Figure 44. SEM photograph of the film produced with 3 J/cm^2 fluence and 1060 nm wavelength.

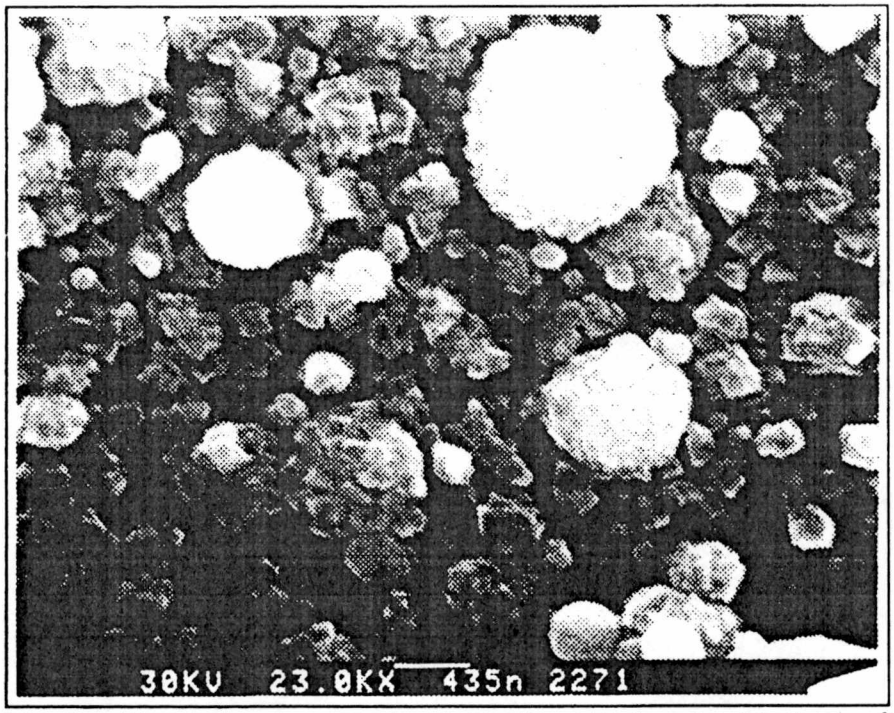

Figure 45. SEM photograph of the film produced with 3 J/cm^2 fluence and 1060 nm wavelength.

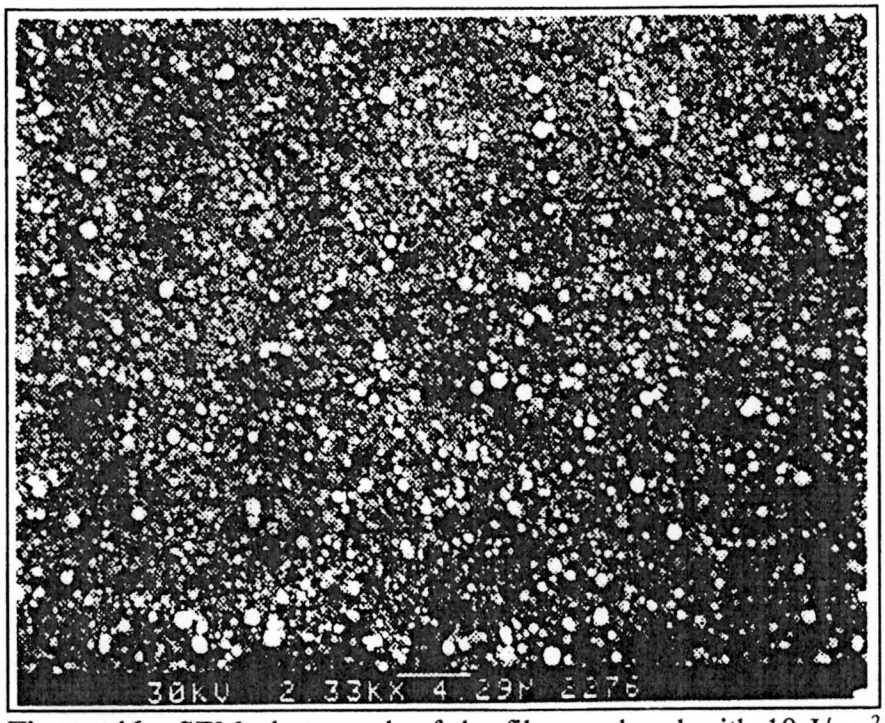

Figure 46. SEM photograph of the film produced with 10 J/cm^2 fluence and 355 nm wavelength.

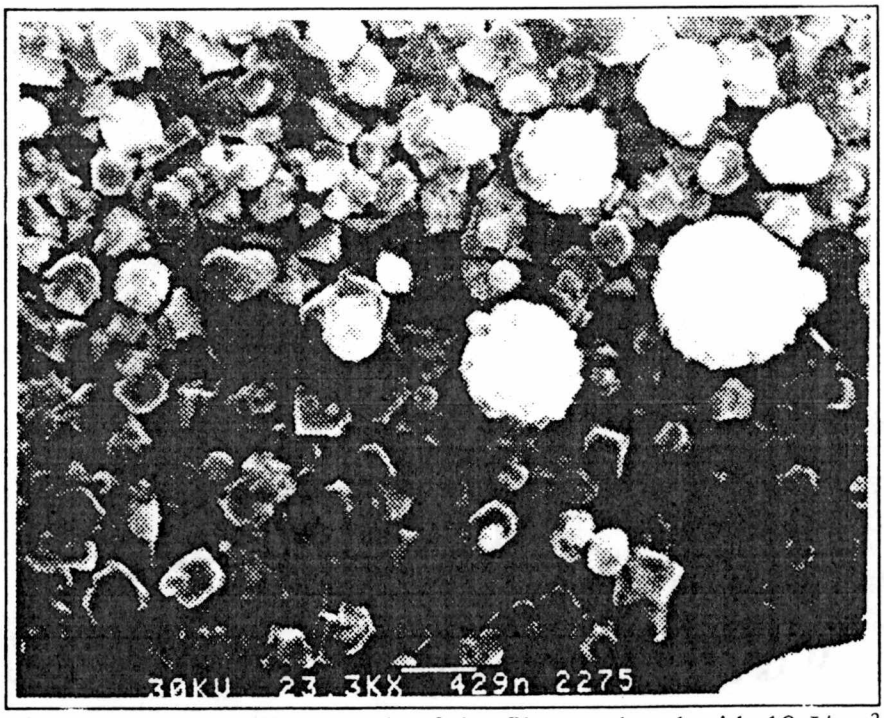

Figure 47. SEM photograph of the film produced with 10 J/cm^2 fluence and 355 nm wavelength.

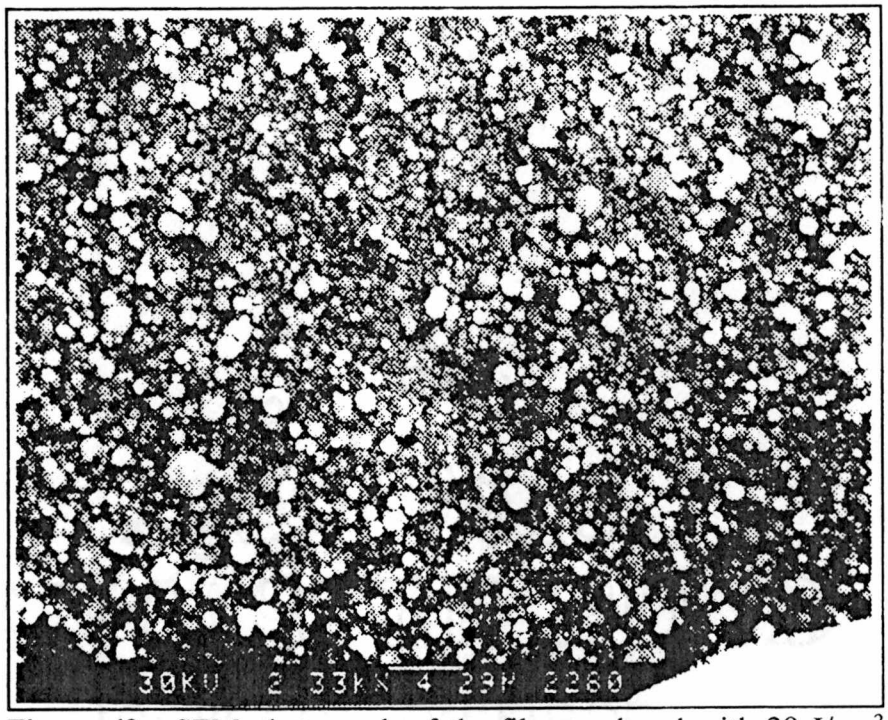

Figure 48. SEM photograph of the film produced with 20 J/cm^2 fluence and 355 nm wavelength.

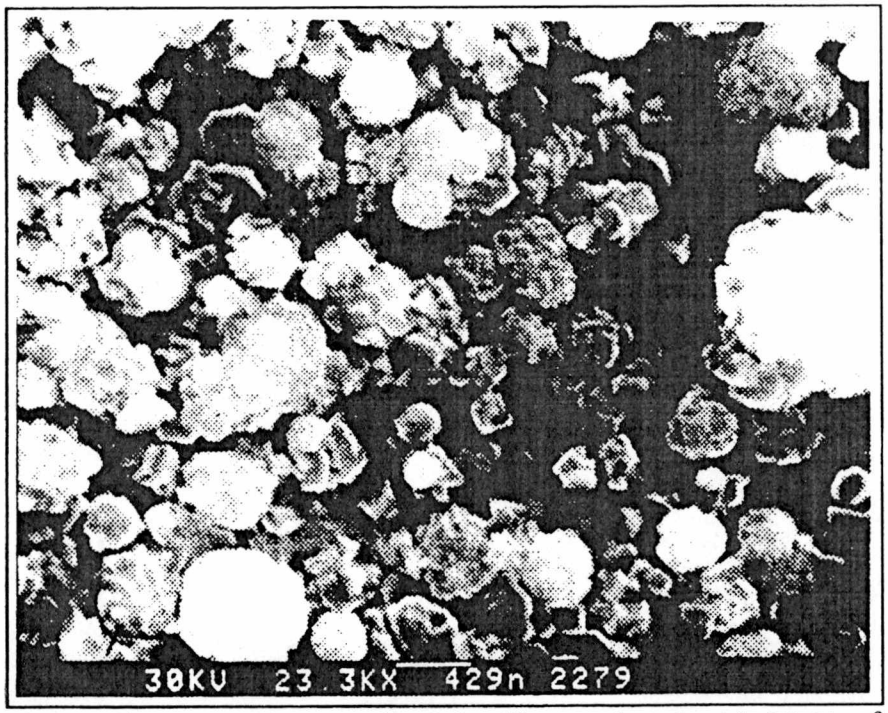

Figure 49. SEM photograph of the film produced with 20 J/cm^2 fluence and 355 nm wavelength.

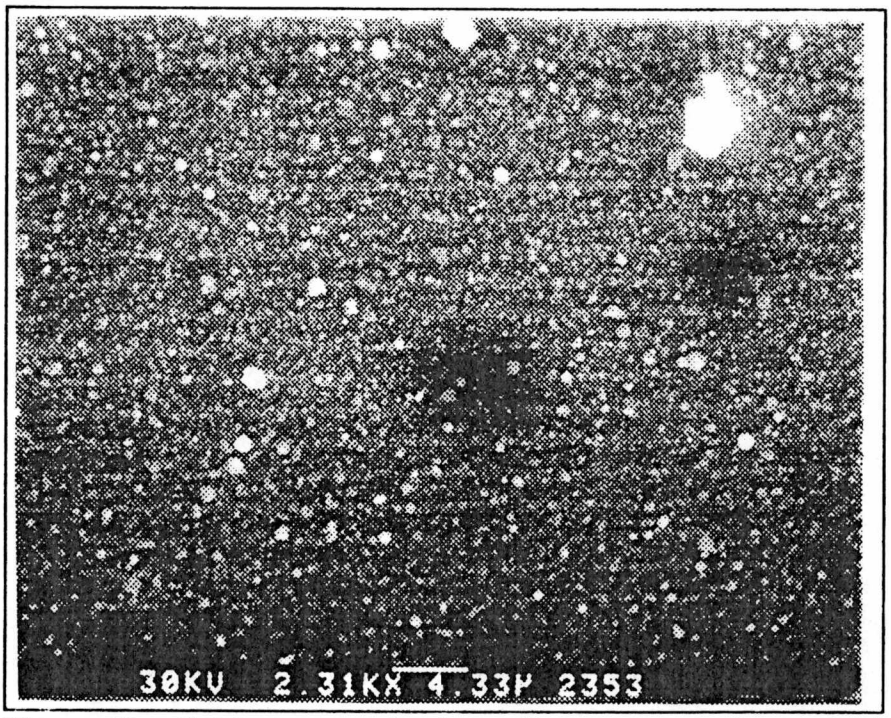

Figure 50. SEM photograph of the film produced with 1 J/cm^2 fluence and 355 nm wavelength.

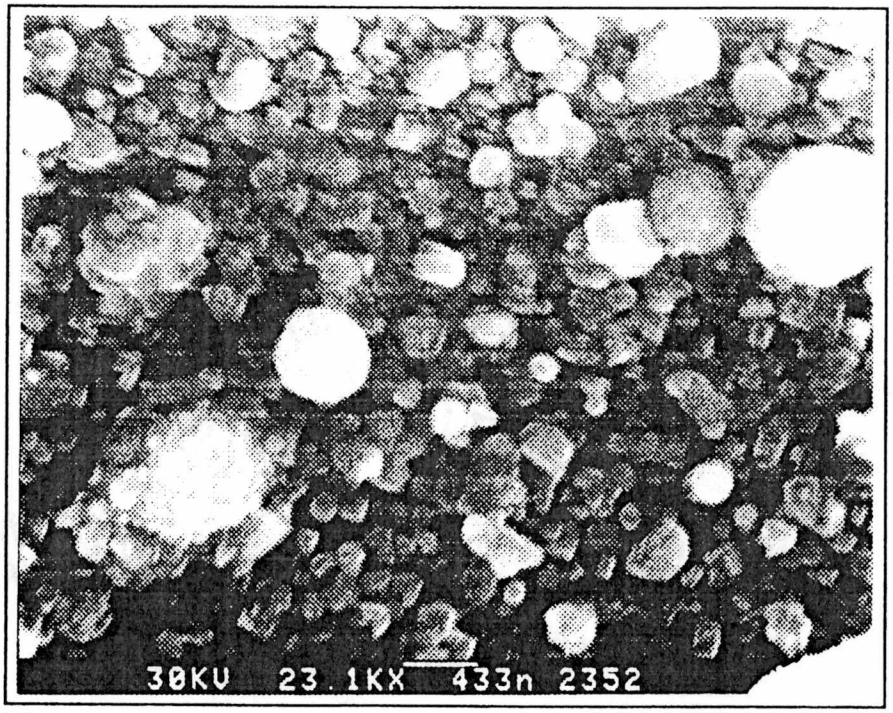

Figure 51. SEM photograph of the film produced with 1 J/cm^2 fluence and 355 nm wavelength.

cause more clusters to be produced, and these photos would support that theory. There are two competing mechanisms for laser ablation at higher fluences: 1) larger particles are produced by an "explosive effect" when the laser beam strikes the target, 2) subsequent absorption of photons breaks up the particles into smaller pieces. The SEM photographs show that the first process may be the dominant one.

CHAPTER 7

CONCLUSIONS

The success of using FT-IR spectroscopy and mass spectrometry as an *in-situ* diagnostic tool for superconducting thin film deposition is reviewed in this section. Suggestions for improving the experiment are also given.

FT-IR Spectroscopy:

1) Can be used to determine if the film is metallic by observing the disappearance of absorption bands as the film is cooled to room temperature. Cannot be used to determine if the film is superconductive.

2) Can show if oxygen is being incorporated into the film by observing an increase in reflectivity.

3) Shows when a sufficient thickness of film has been produced because substrate features are no longer present in the infrared spectra.

4) FT-IR spectroscopy would be most useful when used in conjunction with another device which could successfully monitor ablation parameters.

Mass Spectrometer:

1) Shows that stoichiometry of ablated positive ions in not preserved.

2) Detected no dependence of ablated species with laser wavelength.

3) Suggests that the clusters may be the predominant ablated species, in order to explain differences in film quality when laser wavelength and fluence are varied.

4) Cannot use conventional mass spectrometry to monitor ablation of clusters.

5) SEM photographs support the theory that clusters are the main species produced by laser ablation, since shorter wavelengths and lower fluences produce smaller film particles.

6) Overall, the mass spectrometer is not a good device for monitoring of film deposition.

In order to be able to monitor film deposition *in-situ* and optimize deposition parameters, some other method of detecting ablated particulates will be needed. Perhaps a time-of-flight spectrometer could be used to detect the large clusters, which have been suggested as the main species produced during laser ablation. This new device, when used together with FT-IR spectroscopy, could be used to monitor the deposition process and enable the understanding of the processes involved in producing good quality epitaxial $YBa_2Cu_3O_{7-x}$ superconducting thin films.

BIBLIOGRAPHY

BIBLIOGRAPHY

1. V. Daniel Hunt, Superconductivity Sourcebook, John Wiley and Sons, New York, pp. 2-4 (1989).

2. J.G. Bednorz and K.A. Müller, "Possible High T_c Superconductivity in the Ba-La-Cu-O System," Z. Phys. B- Condensed Matter **64**, pp. 189-193 (1986).

3. M.K. Wu, *et al.*, "Superconductivity at 93 K in a New Mixed-Phase Y-Ba-Cu-O Compound System at Ambient Pressure," Physical Review Letters **58**(9), pp. 908-910 (1987).

4. I-Wei Chen, *et al.*, "Superconductivity and the Tailoring of Lattice Parameters of the Compound $YBa_2Cu_3O_x$," Advanced Ceramic Materials, Special Supplementary Issue: Ceramic Superconductors, vol. 2, no. 3B, American Chemical Society, p. 466 (1987).

5. Frank Herman, Robert V. Kasowski, and William Y. Hsu, "Electronic structure of oxygen-deficient high-T_c superconductors: $YBa_2Cu_3O_x$ $(6 \leq x \leq 8)$," Physical Review B **36**(13), pp. 6904-6905 (1987).

6. D. Dijkkamp, *et al.*, "Preparation of Y-Ba-Cu oxide superconductor thin films using pulsed laser evaporation for high T_c bulk material," Applied Physics Letters **51**(8), pp. 619-621 (1987).

7. X.D. Wu, *et al.*, "Epitaxial ordering of oxide superconductor thin films on (100) $SrTiO_3$ prepared by pulsed laser evaporation", Applied Physics Letters **51**(11), pp. 861-863 (1987).

8. W. Shi, *et al.*, "Influence of substrate temperature on the orientation of $YBa_2Cu_3O_7$ films", Applied Physics Letters **57**(8), pp. 822-824 (1990).

9. S. Witanachchi, *et al.*, "Deposition of superconducting Y-Ba-Cu-O films at 400 °C without post-annealing," Applied Physics Letters **53**(3), p. 235 (1988).

10. John U. Trefiry, "Introduction to Superconductivity", Science and Technology of Thin Film Superconductors, edited by Robert D. McConnell and Stuart A. Wolf, Plenum Press, New York, p. 523 (1989).

11. H.S. Kwok, *et al.*, "Laser evaporation of superconducting and dielectric thin films," Applied Physics Letters **52**(21), pp. 1825-1827 (1988).

12. R.W. Simon, *et al.*, " Growth of High-Temperature Superconductor Thin Films on Lanthanum Aluminate Substrates," Science and Technology of Thin Film Superconductors, edited by Robert D. McConnell and Stuart A. Wolf, Plenum Press, New York, pp. 337-345 (1989).

13. Douglas H. Lowndes, *et al.*, "In-Situ Growth of High Quality Epitaxial $YBa_2Cu_3O_{7-x}$ Thin Films at Moderate Temperatures by Pulsed Laser Ablation," High Temperature Superconductors - Fundamental Properties and Novel Materials Processing, edited by David Christen, Jagdish Narayan, and Lynn Schneemeyer, Materials Research Society, Pittsburgh (1990).

14. G. Koren, *et al.*, "Highly oriented as-deposited superconducting laser ablated thin films of $Y_1Ba_2Cu_3O_{7-\delta}$ on $SiTiO_3$, zirconia, and Si substrates," Applied Physics Letters **53**(23), p. 2330 (1988).

15. X.D. Wu, *et al.*, "Low-temperature preparation of high T_c superconducting thin films," Applied Physics Letters **52**(9), p. 755 (1988).

16. C.H. Chen, R.C. Phillips, and M.P. McCann, "Observation of trapped O_2 in high T_c metal oxide superconductors," Physical Review B **39**, 4, pp. 2744-2747 (1989).

17. C. Deshpandey and R.F. Bunshah, "Synthesis of High Temperature Superconducting Films - Processing Science and Issues," Studies of High Temperature Superconductors: Advances in Research and Applications, vol. 3, edited by Anant Narlikar, Nova Science Publishers, Inc., Commack, N.Y., p. 90 (1989).

18. B. Raveau, C. Michel, and M. Hervieu, "Structural Chemistry of High T_c Superconductors," Studies of High Temperature Superconductors: Advances in Research and Applications, vol. 2, edited by Anant Narlikar, Nova Science Publishers, Inc., Commack, N.Y., p. 8 (1989).

19. C.H. Chen, *et al.*, "In-Situ Monitoring of Laser Ablation of Superconductors," Laser Ablation - Mechanisms and Applications, edited by J.C. Miller and R.F. Haglund, Springer-Verlag Publishing, New York, pp. 16-28 (1991).

20. A. Gupta and B.W. Hussey, "Laser deposition of $YBa_2Cu_3O_{7-\delta}$ films using a pulsed oxygen source," Applied Physics Letters **58**(11), p. 1213 (1991).

21. S.S. Mitra and P.J. Gielisse, "Infrared Spectra of Crystals," Progress in Infrared

Spectroscopy, vol. 2, edited by Herman A. Szymanski, Plenum Press, New York, pp. 70-71 (1964).

22. Jeffrey T. Cheung and Haluk Sankur, "Growth of Thin Films by Laser-Induced Evaporation," CRC Critical Reviews in Solid State and Materials Sciences **15**, 1, p. 81 (1988).

23. X.D. Wu, *et al.*, "Effect of deposition rate on properties of $YBa_2Cu_3O_{7-\delta}$ superconducting thin films," Applied Physics Letters **56**(15), pp. 1481-1483 (1990).

24. C.H. Chen, R.C. Phillips, and P.W. Morrison, "Monitoring of Photodeposited Superconductive Films," Thin Solid Films **218**, p. 299 (1992).

25. Q.Y. Ying, *et al.*, "Study of In-Situ Laser-Deposition of Superconducting Thin Films by In-Situ Resistance Measurement," High-Temperature Superconductors: Fundamental Properties and Novel Materials Processing, edited by David Christen, Jagdish Narayan, and Lynn Schneemeyer, Materials Research Society, Pittsburgh, pp. 494-495 (1990).

26. G. Koren, *et al.*, "Laser wavelength dependent properties of $YBa_2Cu_3O_{7-\delta}$ thin films deposited by laser ablation," Applied Physics Letters **55**(23), pp. 2450-2452 (1989).

27. A.V. Bazhenov, *et al.*, "Infrared Reflectivity, Inelastic Light Scattering and Energy Gap in a Y-Ba-Cu-O Superconductors," Novel Superconductivity, edited by Stuart A. Wolf and Vladimir Z. Kresin, Plenum Press, New York, pp. 893-896 (1987).

28. P. Ganguly, J.R. Fernandes, and C.N.R. Rao, "Infrared Spectra of Superconducting $La_{2-x}Sr_xCuO_4$ and $YBa_2Cu_3O_{7-\delta}$," Phase Transitions **10**, pp. 77-86 (1987).

29. D.M. Back, "Fourier Transform Infrared Analysis of Thin Films," Physics of Thin Films: Thin Films for Advanced Electronic Devices, vol. 15, edited by Maurice H. Francombe and John L. Vossen, Academic Press, Inc., Boston, p. 267 (1991).

30. Zhao Yonggang, *et al.*, "Correlation Between IR Peaks and T_c of $YBa_2Cu_3O_x$," Solid State Communications **68** (9), pp. 847-848 (1988).

31. P. Ganguly, J.R. Fernandes, and C.N.R. Rao, "Infrared Spectra of Superconductive $La_{2-x}Sr_xCuO_4$ and $YBa_2Cu_3O_{7-\delta}$," Phase Transitions **10**, p. 78 (1987).

32. S. Tanaka, *et al.*, "Physical Properties and Superconductivity of Layered Perovskite Oxides," High Temperature Superconductors: Progress in High Temperature Superconductivity - vol. 1, edited by S. Lundqvist, E. Tosatti, M.P. Tosi, and Yu Lu, World Scientific, New Jersey, pp. 120-121 (1987).

33. Yoshio Muto, Norio Kobayashi, and Yasuhiko Syono, "Present Status of High T_c Oxide Superconductivity Studies at Tohoku University," Novel Superconductivity, edited by Stuart A. Wolf and Vladimir Z. Kresin, Plenum Press, New York, p. 790 (1987).

34. M. Rothschild, *et al.*, "Reversible laser chemically induced phase transformations in thin-film $Ba_2YCu_3O_x$ superconductors," Applied Physics Letters **52**(5), p. 404 (1988).

35. L. Lynds, *et al.*, "Superconducting thin films of Y-Ba-Cu-O produced by neodymium:yttrium aluminum garnet laser ablation," Applied Physics Letters **52**(4), p. 321 (1988).

36. G. Koren, A. Gupta, and R.J. Baseman, "Role of atomic oxygen in the low-temperature growth of $YBa_2Cu_3O_{7-\delta}$ thin films by laser ablation deposition," Applied Physics Letters **54**(19), p. 1921 (1989).

37. H.-J. Dietze and S. Becker, "Laser Ionization Mass Spectrometry of $YBa_2Cu_3O_{7-x}$ Superconductors," International Journal of Mass Spectrometry and Ion Processes **82**, p. R2, (1988).

38. Peter R. Griffiths, Chemical Infrared Fourier Transform Spectroscopy, John Wiley and Sons, New York, p. 301 (1975).

39. *Ibid.*, p. 306.

40. R.J. Jakobsen, "Application of FT-IR to Surface Studies," Fourier Transform Infrared Spectroscopy - Applications to Chemical Systems, vol. 2, edited by John R. Ferraro and Louis J. Basile, Academic Press, New York, p. 167 (1979).

APPENDICES

APPENDIX A

RESISTANCE VERSUS TEMPERATURE COMPUTER PROGRAM

```
DECLARE SUB IBFIND (BDNAME$, BD%)
DECLARE SUB ibrd (BD%, rd$)
DECLARE SUB ibwrt (BD%, wrt$)
DECLARE FUNCTION ILFIND% (BDNAME$)
DECLARE FUNCTION FILTER$ (TXT$, FILTERSTRING$)

REM % IS INTEGER, & IS LONG INTEGER, ! IS SINGLE FLOAT,
REM # IS DOUBLE, $ IS STRING

DIM TDATA(100), VDATA(100), VDATA!(100), TDATA!(100)
DIM HPDATA!(100), sensi!(16)
DATA 0.0000001, 0.0000003, 0.000001, 0.000003, 0.000010, 0.000030
DATA 0.00010, 0.00030, 0.001, 0.003, 0.010, 0.03, 0.1, 0.3, 1.0, 3.0
FOR j=0 TO 15: READ sensi!(j): NEXT j
BDNAME$ = "GPIB0"

'       DEV4 is the Hewlett-Packard 3478A multimeter
DEV4$ = "DEV4"
'       DEV8 is the LakeShore Cryotronics 805 temperature controller
DEV8$ = "DEV8"

CALL IBFIND(BDNAME$, UD0%)
UD4% = ILFIND(DEV4$)
UD8% = ILFIND(DEV8$)

PRINT "This program is intended to operate a LAKE SHORE 805;"
PRINT "TEMPERATURE CONTROLLER during the measurement of Tc of"
PRINT "experimental superconductors."
PRINT "This program assumes you have set up instruments properly!"

PRINT "Enter the desired starting temperature.  Your temperature"
INPUT "  must be greater than the current system temperature:", start!
INPUT "Enter the desired ending temperature:", finish!
INPUT "Enter the desired temperature increment between measurements:", incre!
```

```
INPUT "ENTER FILE NAME FOR DATA STORAGE : ", FILNAM$
OPEN FILNAM$ FOR OUTPUT AS #1

'       'F4' SETS HP MULTIMETER TO 4-WIRE OHMS MEASUREMENT
wrt$ = "F4" : CALL ibwrt(UD4%, wrt$)
'       'Z1' SETS HP TO AUTOZERO ON MODE
wrt$ = "Z1" : CALL ibwrt(UD4%, wrt$)
'       'T1' SETS HP TO INTERNAL TRIGGER MODE
wrt$ = "T1" : CALL ibwrt(UD4%, wrt$)
'       'D1' SETS HP TO NORMAL DISPLAY MODE
wrt$ = "D1" : CALL ibwrt(UD4%, wrt$)
'       'RA' SETS HP TO AUTORANGE MODE
wrt$ = "RA" : CALL ibwrt(UD4%, wrt$)
'       'N5' SETS HP TO THE 5.5 DIGIT DISPLAY FOR MAX NOISE REJECTION
wrt$ = "N5" : CALL ibwrt(UD4%, wrt$)
first! = 0
DO UNTIL first! > start!
        wrt$ = "WS" : CALL ibwrt(UD8%, wrt$)
        rd$ = SPACE$(20) : CALL ibrd(UD8%, rd$)
        CLEANNUM$ = FILTER$(rd$, "0123456789.+-")
        SLEEP 5
        first! = VAL(CLEANNUM$)
        PRINT first!
LOOP
test! = 0
old! = first!
WRITE #1, "Temperature (K)              Resistance (Ohms)"

1100    DO UNTIL test! > incre!
                wrt$ = "WS" : CALL ibwrt(UD8%, wrt$)
                rd$ = SPACE$(20) : CALL ibrd(UD8%, rd$)
                CLEANNUM$ = FILTER$(rd$, "0123456789.+-")
                sample! = VAL(CLEANNUM$)
                PRINT sample!
                test! = sample! - old!
        LOOP
test! = 0
old! = sample!
one! = 0
rd$ = SPACE$(20) : CALL ibrd(UD4%, rd$)
CLEANED$ = FILTER$(rd$, "0123456789.+-")
ohm! = VAL(CLEANED$)
SLEEP 5
PRINT sample!, ohm!
```

```
WRITE #1, sample!, ohm!
IF sample! < finish! GOTO 1100
END


FUNCTION FILTER$ (TXT$, FILTERSTRING$) STATIC
      TEMP$ = ""
      TXTLENGTH = LEN(TXT$)
      FOR i = 1 TO TXTLENGTH
            C$ = MID$(TXT$, i, 1)
            IF INSTR(FILTERSTRING$, C$) < > 0 THEN
                  TEMP$ = TEMP$ + C$
            END IF
      NEXT i
      FILTER$ = TEMP$
END FUNCTION
```

APPENDIX B

CALCULATION OF LASER FLUENCE AND TARGET AREA

In order to demonstrate the method used to calculate laser fluence and target area, here is a sample calculation.

The objective is to obtain a fluence of 3 J/cm^2 with a laser energy of 20 mJ:

3 J/cm^2 = 20 x 10^{-3} J/Area

Area = $\pi x^2 + \pi(f\theta)^2$ = 0.00667 cm^2

where $(f\theta)^2$ = [(45 cm)(5 x 10^{-4})]^2 = 5.06 x 10^{-4} cm^2

due to the beam divergence of the laser

$\pi(x^2 + 5.06 \times 10^{-4})$ = 0.00667 cm^2

x = 0.0402 cm

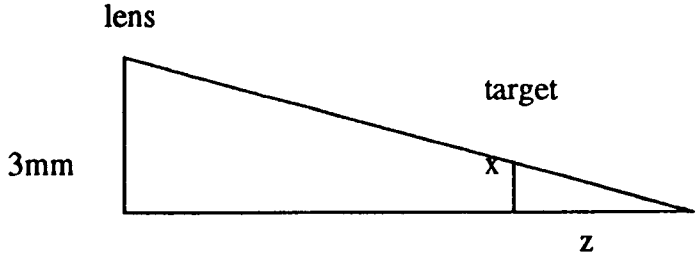

3/450 = x/z

450 mm

150 x = z

z = 6.0 cm

45 cm - 6.0 cm = 39.0 cm from lens to target

39.0 cm - 20.96 cm = 18.0 cm from lens to window

(where 20.96 cm is the distance from the target to the window of the vacuum chamber)

APPENDIX C

RELATIONSHIP BETWEEN SKIN DEPTH AND RESISTIVITY

The infrared spectra obtained in these experiments made use of a Michelson interferometer. A schematic of the instrument is shown below:

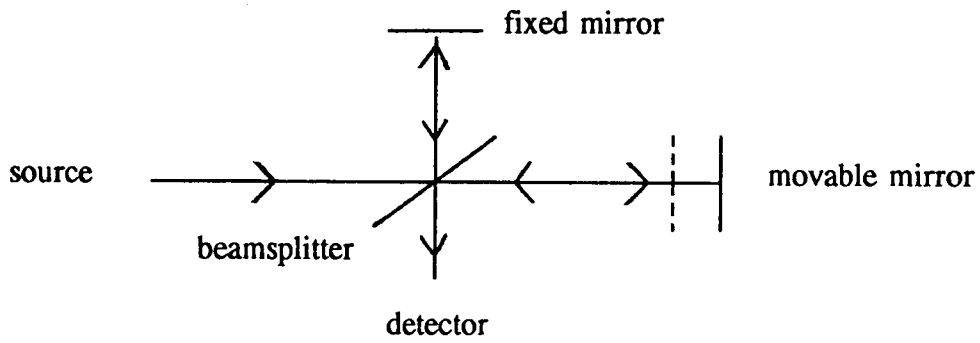

The interferogram is the intensity of light at the detector as a function of the path difference, δ, of the two beams. If the Fourier transform of $I(\delta)$ is taken, then the intensity as a function of wavelength (or wavenumber) is obtained [29].

When the beam of the interferometer strikes the surface of the film, it actually passes through the film and interacts with it and may penetrate to the substrate, and is then reflected back through the film to the detector. Therefore, the procedure used to acquire an interferogram is not strictly reflection spectroscopy, though it more closely resembles that technique than any other [38]. In electrodynamics, resistivity is directly

related to skin depth; therefore, films that are more resistive would allow the IR beam to penetrate farther and films that are less resistive would allow the beam to penetrate less. It is possible that more metallic films (which are less resistive) do not allow the IR beam of the interferometer to reach the substrate, so that the features of the interferogram which seem to be due to the $LaAlO_3$ substrate at low wavenumbers are not present. Generally, the films that demonstrated features of the substrate were not superconductive and therefore, not metallic, and they support this theory. Conversely, films that were superconducting exhibited the substrate features.

Typically, the best FT-IR spectra of surface features are obtained with a high incidence angle and polarized radiation [39]. Also, multiple reflections are often required in order to produce an intense signal [40].

VITA

Angelia Kaye Moore was born in Carrollton, Georgia on September 19, 1968. After graduating from Alcoa High School in Alcoa, TN in 1986, she attended Carson-Newman College in Jefferson City, TN, where she received a Bachelor of Arts with a major in physics and a minor in mathematics in 1990. In that same year, she began graduate studies at the University of Tennessee, Knoxville in physics. Her research began at the Oak Ridge National Laboratory in June 1991 and continued until February 1993. She received a Master of Science in physics from the university in May 1993.